Universidade do Minho
Escola de Engenharia
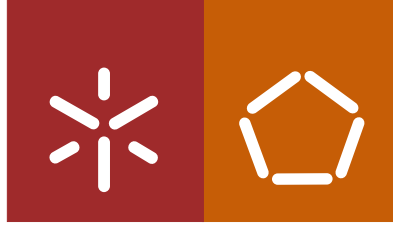
João Miguel Pereira Fidalgo

Development of a water-soluble Dextrin-Amphotericin B formulation for the treatment of Leishmaniasis

outubro de 2018

Universidade do Minho
Escola de Engenharia

João Miguel Pereira Fidalgo

**Development of a water-soluble
Dextrin-Amphotericin B formulation
for the treatment of Leishmaniasis**

Dissertação de Mestrado
Mestrado Integrado em Engenharia Biomédica
Ramo de Engenharia Clínica

Trabalho realizado sob orientação do
Professor Doutor Francisco Miguel Portela da Gama
e da
Professora Doutora Ana Maria Tomás

outubro de 2018

DECLARAÇÃO

Nome: João Miguel Pereira Fidalgo

Endereço eletrónico: joao.fidalgo.10@gmail.com

Telefone: 918348199

Número do Bilhete de Identidade/Cartão de Cidadão: 14612240

Título da dissertação: Development of a water-soluble Dextrin-Amphotericin B formulation for the treatment of Leishmaniasis

Orientador(es):

Professor Doutor Francisco Miguel Portela da Gama

Professora Doutora Ana Maria Tomás

Ano de conclusão: 2018

Designação do Mestrado: Mestrado Integrado em Engenharia Biomédica, Ramo de Engenharia Clínica

Universidade do Minho, ___/___/_____

Assinatura: _____

Agradecimentos

É com imenso orgulho que vejo chegar ao fim o meu percurso académico, um percurso que fez de mim uma pessoa mais resiliente, disciplinada e autónoma. Assim sendo, gostaria de agradecer a todas as pessoas que tornaram possível a concretização desta etapa da minha vida, que culminou com a realização desta dissertação de mestrado.

Em primeiro lugar, gostaria de agradecer ao Professor Miguel Gama pela oportunidade concedida, por me permitir realizar um trabalho da minha área de interesse e por toda a experiência que me permitiu adquirir. Agradeço ainda pelo acompanhamento e confiança que me deu ao longo da realização deste trabalho.

Agradecer também à Professora Ana Tomás pela oportunidade de integrar um laboratório numa unidade de investigação de renome mundial, o Instituto de Investigação e Inovação em Saúde da Universidade do Porto (I3S). Agradeço também por todos os conselhos e orientações que me deu ao longo deste último ano.

Agradecer ao professor Pier Parpot, pelo apoio e disponibilidade constantes na realização das análises de HPLC. Sem dúvida que a sua ajuda foi fundamental para atingir um dos principais objetivos deste trabalho.

Quero agradecer a todos os membros do grupo de investigação 'Molecular Parasitology' do I3S por me integrarem como um de vós durante a minha curta estadia neste grupo de investigação. Em especial, gostaria de agradecer à Tânia e à Gina, por todos os conselhos e ensinamentos que me transmitiram, bem como por todo o tempo de que abdicaram para me ajudar.

Agradeço também a todos os membros do grupo de investigação FUNCARB do CEB por este último ano, em que fui muito bem acolhido neste laboratório. Em geral, gostaria de agradecer à Alexandra, Cecília, Daniela, Ana Cristina e Francisco por toda a ajuda que me deram. Em especial, gostaria de agradecer ao Ricardo por me ter supervisionado e orientado mais de perto, estando sempre disponível para me ajudar.

Quero agradecer aos grandes amigos que tive oportunidade de fazer em Braga. Ao Luís e ao Gil, pelo vosso companheirismo e amizade, bem como por todas as horas de palhaçada, bebedeira e estudo que passamos juntos. Ao Vítor, pela tua grande amizade. Foste como um irmão para mim, sempre estiveste disponível para me ouvir e ajudar. Aquele 4° Esquerdo será sempre memorável, por tudo o que fizemos dele. Agradecer ainda à Margarida, por todas as conversas que tivemos, por ser a nossa 'Mãe', por estar sempre disponível para vir jantar e estar connosco.

Quero agradecer, do fundo de coração, à minha namorada Mafalda, uma das pessoas mais incríveis que já conheci. És uma pessoa tão única, carinhosa, lutadora, sorridente, com uma aura tão especial. Foste um dos meus principais pilares, nunca me deixaste ir a baixo, nunca desististe de mim, agradeço-te por todo o amor e amizade que temos partilhado e continuaremos a partilhar. Sem ti, tudo seria mais difícil.

Por fim, gostaria de deixar um agradecimento, mais importante do que qualquer outro, aos meus pais. Vocês são, sem sombra de dúvidas, o maior reflexo daquilo que eu pretendo ser. Sem o vosso apoio, amor e esforço diário, nada disto seria possível. Agradeço-vos por todos os esforços que fizeram e fazem por mim, por me tornarem na pessoa que sou hoje e por acreditarem em mim. Agradeço também à minha irmã Mariana, por todo o companheirismo e amor que partilhamos, na esperança de que saibas que tens em mim o teu melhor amigo.

A todos vós, o meu sincero e profundo obrigado!

Resumo

A leishmaniose, uma doença potencialmente fatal causada por parasitas de *Leishmania*, tem sido classificada como uma das doenças tropicais mais negligenciadas, embora existam atualmente 12 milhões de pessoas infetadas, maioritariamente em países pobres e subdesenvolvidos. Atualmente não existem vacinas eficazes para a prevenção da leishmaniose humana e, por conseguinte, o controlo da doença depende de quimioterapia. A Anfotericina B (AmB) é o fármaco mais recomendado, mas apresenta grandes desvantagens como baixa solubilidade em água e elevada toxicidade. Para contornar estes problemas, têm vindo a ser desenvolvidas formulações lipossomais e dispersões micelares. Apesar de estarem no mercado, estes produtos apresentam grandes limitações clínicas ou um custo elevado, limitando o seu uso a nível global. Os sistemas de libertação de AmB à base de polissacarídeos têm emergido como um tratamento alternativo, sendo desenvolvidos através de uma modificação estrutural do polissacarídeo (oxidação) que permite a ligação covalente do fármaco. Contudo, estudos anteriores do grupo (dados não publicados) mostraram que as modificações químicas são dispensáveis. Neste trabalho, o dextrino é proposto como um polissacarídeo adequado para o desenvolvimento de uma formulação de AmB. Uma formulação de Dextrino-AmB foi produzida através de um *self-assembling* por interações fracas, com um rendimento global de 71.1 %. A nanoformulação desenvolvida apresentava uma forma esférica em solução aquosa, com um diâmetro médio de 244 nm (NTA) a 460 nm (DLS). Um método de HPLC-MS foi desenvolvido e permitiu determinar um rendimento de recuperação e um conteúdo de AmB de 134 % e 37.62 %, respetivamente. A nanoformulação não apresentou citotoxicidade *in vitro* para BMMϕ. Para além disso, ensaios *in vitro* contra promastigotas axénicos e amastigotas intramacrofágicos de *Leishmania* demonstraram uma promissora capacidade anti-leishmania, semelhante à exibida pela AmB livre.

Palavras-Chave: Leishmaniose; dextrino; anfotericina B; nanopartículas

Abstract

Leishmaniasis, a life-threatening disease caused by *Leishmania* parasites, has been classified as one of the most neglected tropical diseases, even though there are currently around 12 million people infected, mainly in poor and less developed countries. Nowadays, there are no effective vaccines to prevent human leishmaniasis and thus, the disease control relies on chemotherapy. Amphotericin B (AmB) is the most recommended drug but presents some major drawbacks, such as low water solubility and high toxicity. To circumvent these issues, liposomal formulations or micellar dispersions have been developed. Despite being on the market, these products still present either major clinical limitations or a high-cost, hampering its use worldwide. Polysaccharide-based AmB delivery systems have emerged as an alternative treatment. Those formulations are developed through a polysaccharide backbone modification (oxidation) that allows a drug covalent conjugation. However, previous studies (unpublished data) done in our research group showed that chemical modifications are dispensable. In this work, dextrin is proposed as a suitable polysaccharide for the development of an AmB formulation. A Dextrin-AmB formulation was produced through a self-assembling process involving weaker forces, with an overall yield of 71.1%. The developed nanoformulation presented a spherical form when in aqueous solution, with a mean diameter of 244 nm (NTA) to 460 nm (DLS). An HPLC-MS method was developed and allowed to determine an AmB recovery efficiency (RE) and content of 134 % and 37.62 % (w/w), respectively. The nanoformulation did not present *in vitro* cytotoxicity to BMMɸ. Moreover, *in vitro* assays against *Leishmania* axenic promastigotes and intramacrophagic amastigotes showed a promising anti-leishmanial capacity, similar to the one displayed by free-AmB.

Keywords: Leishmaniasis; dextrin; amphotericin B; nanoparticles

Index

List of Figures

List of Tables

List of Abbreviations

Abbreviation	Designation
AmB	Amphotericin B
BMMΦ	Bone Marrow-derived Macrophages
CL	Cutaneous Leishmaniasis
Cryo-SEM	Cryo-Scanning Electron Microscopy
DAPI	4',6-diamidino-2-phenylindole
DEG	Diethylene glycol
DLS	Dynamic Light Scattering
DMEM	Dulbecco's Modified Eagle Medium
DMSO	Dimethyl sulfoxide
DNA	Deoxyribonucleic Acid
DP	Degree of Polymerization
EDS	Energy Dispersive X-Ray Spectroscopy
ESI	ElectroSpray Ionization
FBS	Fetal Bovine Serum
FDA	Food and Drug Administration
FTIR	Fourier-transform Infrared Spectroscopy
GRAS	Generally Recognized as Safe
HCS	High-content Screening
HEPES	(4-(2-hydroxyethyl)-1-piperazineethanesulfonic acid)
HIV	Human Immunodeficiency Virus
HPLC	High Performance Liquid Chromatography
KHP	Potassium hydrogenphthalate
LCCM	L929 Cell-conditioned media
M-CSF	Macrophage colony-stimulating factor
MA	Meglumine Antimoniate
MAA	Medium for axenically grown amastigotes
MCL	Mucocutaneous Leishmaniasis

MEM	Minimum Essential Medium Non-Essential
MPS	Mononuclear Phagocyte System
MS	Mass Spectrometer
Mw	Molecular weight
NTA	Nanoparticle tracking analysis
NTD	Neglected Tropical Disease
PDA	Photodiode Array
PDI	Polydispersion Index
PEG	Polyethylene glycol
PES	Polyethersulfone
PFA	Paraformaldehyde
PKDL	Post Kala-azar Dermal Leishmaniasis
PLGA	Poly Lactic-co-glycolic acid
RPMI	Roswell Park Memorial Institute
RE	Recovery Efficiency
SIM	Selected Ion Monitoring
VL	Visceral Leishmaniasis
WHO	World Health Organization

1. Introduction

1.1 Leishmaniasis

1.1.1   History and taxonomy

In the beginning of the XIX century, Leishman and Donovan identified and described, the parasites that caused a life-threatening disease, nowadays known as leishmaniasis. These parasites were named as *Leishmania* by Ross in 1903 (Herwaldt, 1999; Steverding, 2017) and to date, 20 species of *Leishmania* are considered pathogenic to humans (Iborra *et al.*, 2018), with the main ones described in Table 1.

Table 1- Clinical forms and geographical distribution of the main *Leishmania* species pathogenic to humans. Adapted from Burza *et al.* (2018)

Species	Clinical Form	Geographical Distribution
Subgenus *Leishmania,* Old World		
L. donovani	VL*; PKDL*	India, Bangladesh, Ethiopia, Sudan and South Sudan
L. tropica	CL*; VL (rare)	Eastern Mediterranean, Middle East, North-eastern and Southern Africa
L. aethiopica	CL; DCL*	Ethiopia and Kenya
L. major	CL	Iran, Saudi Arabia, North Africa, Middle East, Central Asia and West Africa
L. Infantum	VL; CL	China, Southern Europe, Brazil, and South America for VL and CL; Central America for CL
Subgenus *Leishmania,* New World		
L. mexicana	CL; DCL	South America
L. amazonensis	CL; DCL	South America
Subgenus *Viannia,* New World		
L. braziliensis	CL; MCL*	South America
L. guyanensis	CL; MCL	South America

*Note: VL, visceral leishmaniasis; CL, cutaneous leishmaniasis; MCL, mucocutaneous leishmaniasis; DCL, diffuse cutaneous leishmaniasis; PKDL, post kala-azar leishmaniasis.

Protozoan parasites of the genus *Leishmania* are a diversified group of pathogenic organisms that taxonomically belong to the order of

Kinetoplastida and the family *Trypanosomatidae.* Two subgenera emerge from the *Leishmania* genus: *Leishmania (Leishmania) spp*. and *Leishmania (Viannia) spp. (Lukes et al., 2014).*

1.1.2 Morphology and life cycle

Leishmania parasites are transmitted to mammals by the bite of a female sand fly (Bates & Rogers, 2004), a biological vector that belongs to the subfamily *Phlebotominae*. Only two genus of these insects are capable of transmitting the parasite: *Phlebotomus spp.*, present in the Old World*,* and *Lutzomyia spp*., present in the New World (Banuls *et al.*, 2007; Kaye & Scott, 2011). Other less significant ways of transmission that may occur are organ transplantation, congenital transmission or blood transfusions by needle sharing (Oryan & Akbari, 2016; Pavli & Maltezou, 2010).

During its life cycle, *Leishmania* parasites exhibit two distinct morphological forms: promastigote, the extracellular form found in the midgut of the sand fly, and amastigote, the intracellular mammalian form that lives inside the cells of the mononuclear phagocyte system (MPS) (e.g. macrophages, neutrophils and dendritic cells) (Banuls *et al.*, 2007; Handman & Bullen, 2002; Nagle *et al.*, 2014).

Promastigotes have a small size, between 10 to 20 μm, and an elongated flagellum, as seen in Figure 1A. Promastigotes undergo a differentiation process called metacyclogenesis in the digestive tract of the sand fly. In this process, procyclic promastigotes, a non-infective and weakly motile form, multiplies during a few days. Afterwards, the replication process is slowed and the parasite differentiates into metacyclic promastigotes, which are highly infective (Bates, 2007; Kamhawi, 2006).

Amastigotes have a round form and lose the flagellum, as shown in Figure 1B. This intracellular form resides within the harsh environment of the macrophage phagolysosome, where it survives and replicates (Bates, 2007; McConville *et al.*, 2007).
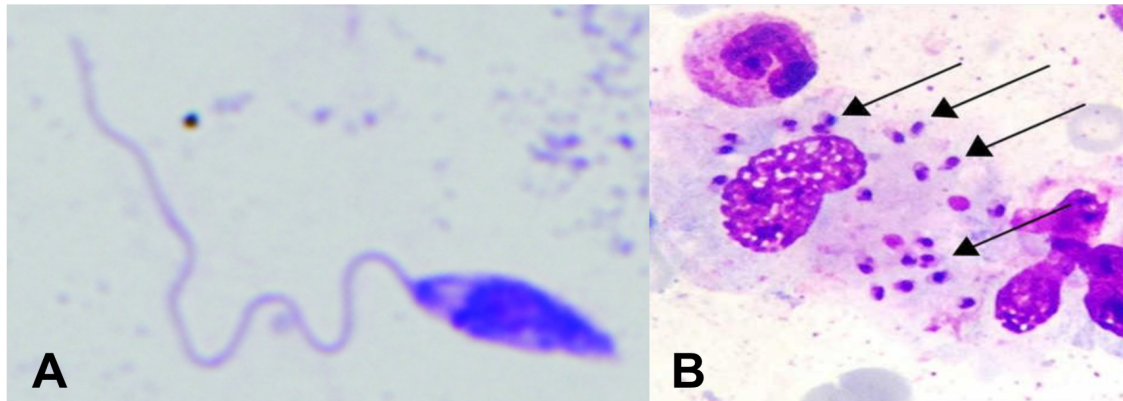
Figure 1- *Leishmania* parasite morphological forms: (A) *Leishmania* promastigotes. Adapted from Sadlova *et al.* (2017); (B) *Leishmania* amastigotes, represented by black arrows. Adapted from Noronha & Fock *(2018)*.

The parasite life cycle is digenetic, starting during a blood meal of a *Leishmania*-infected sand fly. When feeding from a vertebrate host (mainly humans and dogs), the insect introduces saliva containing metacyclic promastigotes *(Ashford, 1996; Gramiccia & Gradoni, 2005; WHO, 2010)*. This triggers an immune response that results in the phagocytosis of the parasite by immune cells. Once inside the phagocytic cell, the promastigotes are exposed to different stimuli (e.g. changes in temperature and acidic pH), that lead to the differentiation into amastigotes. This new parasite form is resistant to the phagolysosomal acidic and enzymatic conditions and thus, the parasite is able to proliferate within the phagolysosome. Such replication may result in the lysis of the MPS cells and consequent infection of other phagocytes (Bates, 2007; Bruni *et al.*, 2017; Lodge & Descoteaux, 2008; McConville *et al.*, 2007; Moradin & Descoteaux, 2012; Rogers *et al.*, 2004). *Leishmania* life cycle is initiated, again, when an uninfected *Phlebotominae* insect takes a blood meal from an infected host ingesting free amastigotes or infected macrophages (Figure 2, in red arrows). (Bates, 2007; Esch & Petersen, 2013; Nagle *et al.*, 2014).
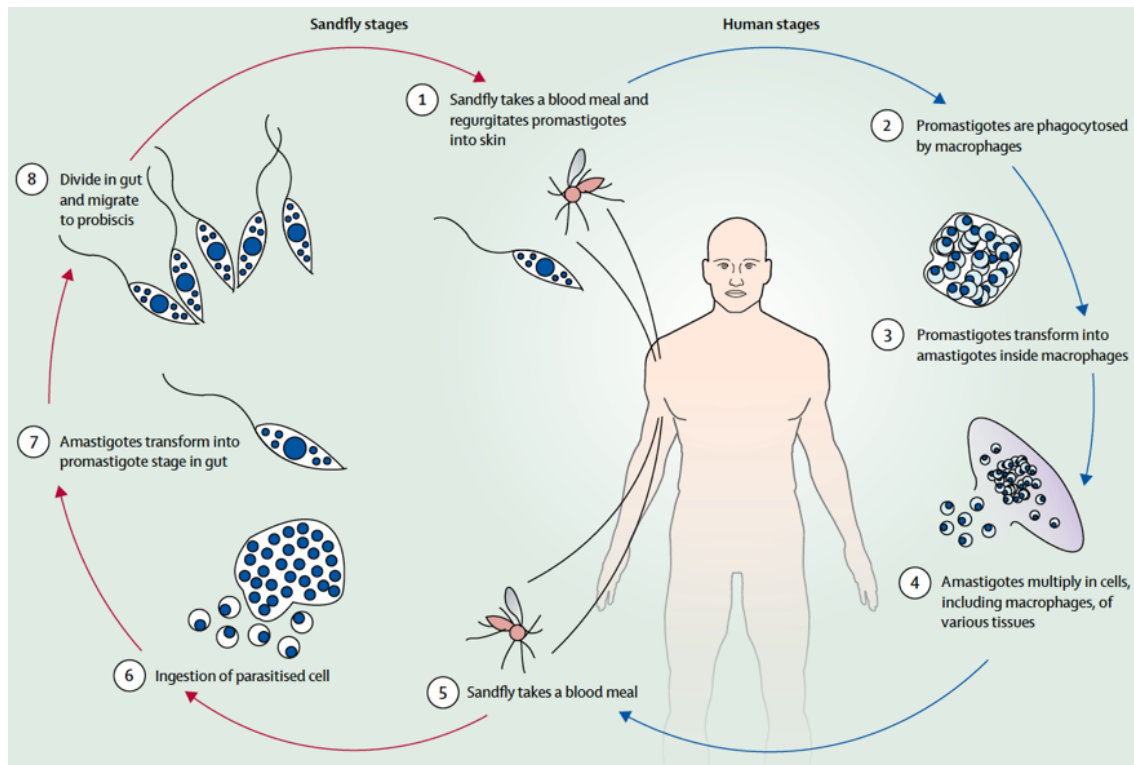
Figure 2- *Leishmania* parasite life cycle. Adapted from Reithinger *et al.* (2007).

1.1.3   Epidemiology and geographical distribution

Leishmaniasis has the ninth largest infectious disease burden worldwide and is already reported as endemic in 97 countries. The bigger part of these are developing countries, where poverty prevails. Despite this, it is still categorized as a neglected tropical disease (NTD) (Alvar *et al.*, 2012; WHO, 2017b). Moreover, global authorities estimate that there are 12 million people infected worldwide, with 1.5 to 2 million new cases and 50 000 deaths reported every year. Although elimination strategies have been engineered and applied, there are 1 billion people at risk of contracting one of the clinical forms of the disease (Alvar *et al.*, 2012; Burza *et al.*, 2018; Oryan & Akbari, 2016; Torres-Guerrero *et al.*, 2017; WHO, 2017a). The actual numbers are thought to be even bigger, due to the known under-reporting in numerous locations worldwide (Alvar *et al.*, 2012).

Currently, its geographical distribution is broader than as ever been, reaching four continents (Figure 3A and 3B). Leishmaniasis is mainly present in South and Central America, Eastern Mediterranean, Southeast Asia and East Africa.

4

Figure 3- Geographical distribution of reported cases, in 2015, of: (A) Cutaneous and mucocutaneous leishmaniasis; (B) Visceral Leishmaniasis. Adapted from WHO (2017c).

The main risk factors that contribute to an ever-growing dissemination of leishmaniasis are: environmental, such as deforestation or climatic and ecological changes, that lead to a wider vector distribution and an increase of reservoir hosts numbers; migratory movements following a conflict, leading to the establishment of non-immune populations into endemic areas; socio-economic status, not only because the poorest populations tend to have difficult access to leishmaniasis treatments but also because they live in rural areas, where the sand fly has the optimal conditions to develop (e.g, humidity, subsoil water, high rubbish content or livestock) (Al-Salem *et al.*, 2016; Bashaye *et al.*, 2009; Belen & Alten, 2006; Dujardin *et al.*, 2008; Pascual Martinez *et al.*, 2012). Additionally, HIV/Leishmaniasis co-infected patients display a role in disease dissemination by needle-sharing (WHO, 2018).

1.1.4   Clinical Manifestations

The clinical manifestation of leishmaniasis depends on the dynamic interplay of three factors: parasite and vector characteristics and host immunologic response. *Leishmania* species have different mechanisms of pathogenicity or virulence, suggesting that the parasite dissemination within the human body is correlated with the parasite characteristics. Similarly, some genus of *Phlebotomus* or *Lutzomyia* can only sustain the development

of one *Leishmania* strain, while others are considered permissive vectors, allowing the growth of more than one parasite specie. The host's immune capacity to develop a protective response plays a decisive role in the clinical outcome. This is clearly seen in immunocompromised individuals, which sometimes develop aggressive and chronic states of the disease that would otherwise self-heal (Burza *et al.*, 2018; Colmenares *et al.*, 2002; G. Gupta *et al.*, 2013; Saporito *et al.*, 2013; Weigle & Saravia, 1996).

Three clinical forms of leishmaniasis can be identified in humans: cutaneous leishmaniasis (CL), mucocutaneous leishmaniasis (MCL), visceral leishmaniasis (VL).

1.1.4.1 Cutaneous leishmaniasis

Most of *Leishmania* species that are pathogenic to humans cause CL, as seen in Table 1. Although this clinical form is not life-threatening, it causes one or multiple nodules in the patient's skin (Figure 4A), that will ulcerate over-time. In most cases, these ulcers self-heal, yet patients often remain with a permanent scar (de Vries *et al.*, 2015; Lakhal-Naouar *et al.*, 2015; WHO, 2010). A more extreme and chronic form of CL can also occur, diffuse cutaneous leishmaniasis (DCL), caused by *L. aethiopica*, characterized by the dissemination of the lesion to multiple skin areas (Bennis *et al.*, 2017; Murray *et al.*, 2005; WHO, 2010).

1.1.4.2 Mucocutaneous leishmaniasis

This clinical form is characterized by progressive ulcers in mucosal membranes (Figure 4B), such as the oronasal or buccal, sometimes reaching the pharynx and the larynx (Murray *et al.*, 2005). MCL normally causes disfiguration due to its destructive effects, ultimately leading to the collapse of some of the above mentioned organs. Usually, MCL cases arise from inefficacious or inexistent CL treatments, with the exception of immunocompromised individuals, who have more predisposition to develop this form of leishmaniasis (Llanos-Cuentas *et al.*, 1997; Strazzulla *et al.*, 2013; WHO, 2010).

1.1.4.3 Visceral leishmaniasis

Although most of VL infections are asymptomatic, this is considered the most acute clinical form of the disease and can be fatal if left untreated (Alves *et al.*, 2018; Burza *et al.*, 2018; WHO, 2010). Also known as kala-azar, VL is caused by *L. infantum* and *L. donovani* in the New World, while *L. chagasi* is responsible for most of the cases in the Old World (Karimi *et al.*, 2016; WHO, 2010). VL is characterized by a dissemination of *Leishmania* species to internal organs, such as the liver, spleen, bone marrow or the lymph nodes, causing swelling (e.g., spenomegaly or hepatomegaly) (Figure 4C) (S. Gupta *et al.*, 2010). In VL patients the most common symptoms are fever, anemia and weight loss or asthenia (Torres-Guerrero *et al.*, 2017; WHO, 2010). When the disease progresses and is left untreated, the death rate increases to 85 %, due to multisystem failure, internal hemorrhages or other severe infections (Stockdale & Newton, 2013; Torres-Guerrero *et al.*, 2017).

Another form of VL may occur years after a "successful" treatment, this clinical form is named post kala-azar dermal leishmaniasis (PKDL). The latter causes skin or limbs lesions, such as nodular or papular rashes (Figure 4D) in the infected patients and has been described in some South Asian and East African countries where, in some cases, the disease self-heals (Mukhopadhyay *et al.*, 2014; Zijlstra, 2016).
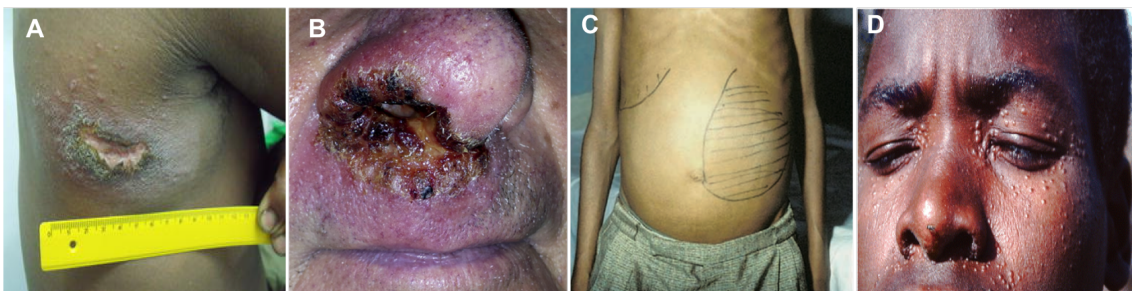
Figure 4- Clinical manifestations of leishmaniasis: (A) Cutaneous leishmaniasis. Adapted from de Vries *et al.* (2015); (B) Mucocutaneous leishmaniasis. Adapted from Burza *et al.* (2018); (C) Visceral leishmaniasis. Adapted from Murray *et al.* (2005); (D) Post kala-azar leishmaniasis. Adapted from Zijlstra (2016).

1.2 Treatment of leishmaniasis

Leishmaniasis prevalence is higher in poor population of sub-developed regions, which raises a plethora of challenges to the prevention and treatment of the disease. Due to economical restrictions and remote localization, these populations have limited access to diagnosis tools and/or affordable treatment, making the control of this disease troublesome (Ghorbani & Farhoudi, 2018; Okwor & Uzonna, 2016; Tiuman *et al.*, 2011). Despite the well-established knowledge and the recent advance in our understanding of leishmanial biology, some aspects of this disease remain enigmatic and therefore the current control or treatment strategies are rather inadequate (Kaye & Scott, 2011; Olivier, 2011). Due to the lack of effective human vaccines to prevent leishmaniasis, the management/cure relies on chemotherapy. However, a greater part of these drugs have aggressive side effects, limited effectivity and demand rigorous regimens of treatment, which can further result in the emergence of parasite resistances (Ghorbani & Farhoudi, 2018; Gillespie *et al.*, 2016; Ponte-Sucre *et al.*, 2017; Tiuman *et al.*, 2011). It is, therefore, urgent to develop new drugs or pharmaceutical formulations that provide improved efficiency at a lower cost, in order to control leishmaniasis at a worldwide scale.

1.2.1 Current treatment options

1.2.1.1 Pentavalent antimonials

The first reports of antimonials use in the treatment of leishmaniasis date back to 1915. Pentavalent antimonials are still considered as first-line choice to treat the main clinical forms of leishmaniasis (e. g., CL and VL) (Frézard *et al.*, 2017; Nagle *et al.*, 2014). Their mechanism of action remains unclear, although they are suspected to act as prodrugs that shift into a toxic form *in vivo* (Frézard *et al.*, 2017).

Meglumine antimoniate (MA) (Glucantime®) and sodium stibogluconate (Pentostam®) are two approved drugs widely used around the globe with the exception of specific regions, namely: hyper-endemic areas (e, g. Bihar State, India) where the development of resistances led to

8

the failure of treatment in 60 % of the cases and Europe, where these drugs have been replaced by Ambisome®, which has a higher cost-efficacy ratio compared with pentavalent antimonials (de Menezes *et al.*, 2015; Frézard *et al.*, 2017; Nagle *et al.*, 2014; Rosenthal *et al.*, 2009). Pentavalent antimonials have a low cost and are usually administered via intralesional injection, promoting higher drug bioavailability where of interest. On the other hand, these require a prolonged and painful treatment and present severe side effects (e, g. arthralgia, abdominal pain or possible fatal cardiac arrhythmias) due to its cardiotoxicity (Ghorbani & Farhoudi, 2018; Nagle *et al.*, 2014).

1.2.1.2 Pentamidine

Pentamidine (Pentacarinat®) is a diamidine used as second-line treatment of VL, in the antimony-resistant areas, such as the previously stated Bihar State, in India. Its mechanism of action relies on affecting the parasite kinetoplast, promoting a programmed cell death (Nagle *et al.*, 2014; No, 2016).

Although it is effective in low doses and has enabled to circumvent the resistance problems of antimonials, pentamidine presents highly toxic effects and can cause diabetes mellitus, hypotension or myocarditis, while being less efficient when compared to Amphotericin B (AmB) (de Menezes *et al.*, 2015; Nagle *et al.*, 2014; O. P. Singh *et al.*, 2016).

This drug is recommended for combined therapy in HIV-Leishmaniasis co-infected patients and as a combined therapy (Nagle *et al.*, 2014; No, 2016).

1.2.1.3 Paromomycin

Paromomycin is an antibiotic isolated from *Streptomyces krestomuceticus* that presents anti-leishmanial activity. It is though that protein synthesis inhibition is the main mechanism of action (Chawla *et al.*, 2011).

This drug has shown positive effects in the treatment of CL and VL and is mainly used as parental or topical formulation, as to overcome its poor

oral absorption (Nagle *et al.*, 2014; Tiuman *et al.*, 2011). Some studies have concluded that paromomycin has similar efficacy in relation to AmB and to MA, but requiring a longer period than the latter to clinically heal CL (Armijos *et al.*, 2004; Sundar *et al.*, 2007). Paromomycin treatments are low-cost and this drug has also bactericidal activity; however, its parenteral formulations cause pain at the injection site and side effects, such as increased bilirubin values or nephrotoxicity and ototoxicity (de Menezes *et al.*, 2015; Nagle *et al.*, 2014).

1.2.1.4 Miltefosine

Miltefosine (Impavido™) is an alkylphosphocholine drug that has shown *in vitro* anti-leishmanial activity. Its mechanism of action is based on the modification of phospholipid metabolism, which causes *Leishmania* apoptosis (Lux *et al.*, 1996).

This was the first marketed oral drug to treat VL and have some advantages, such as effectiveness in the CL and VL treatment, easiness of administration, good oral absorption and reduced side effects. (Nagle *et al.*, 2014; Tiuman *et al.*, 2011). However, oral Miltefosine also exhibits some disadvantages: a 28-day treatment period is required, which could lead to a decrease in patient compliance; teratogenic potential, which could comprise its use by patients that are pregnant or in child-bearing-age and high probability of developing parasite resistances, since the drug has a 7-days half-life (No, 2016; O. P. Singh *et al.*, 2016; Tiuman *et al.*, 2011).

1.2.1.5 Amphotericin B

Amphotericin B (AmB) is a polyene antibiotic, isolated from *Streptomyces spp..* Despite being initially used for the treatment of fungal infections (Charvalos *et al.*, 2006; Nagle *et al.*, 2014), it has shown to have anti-leishmanial activity. This is thought to be related with the affinity to the parasite cell membrane sterols, namely ergosterol and cholesterol. By interacting with ergosterol, AmB promotes the formation of pores that will lead to parasite membrane disruption and consequent death by leakage of

intracellular ions. It is also thought that AmB interacts with the cholesterol of host macrophages membrane, hindering the binding of the parasite to the macrophage (Baginski *et al.*, 2006; Baran *et al.*, 2009; Mesa-Arango *et al.*, 2012).

AmB is currently used as first-line treatment in some areas of India, where antimonial resistance has high incidence, and as second-line treatment for VL and MCL in patients with HIV-Leishmaniasis co-coinfection (Ehrenfreund-Kleinman *et al.*, 2002; O. P. Singh *et al.*, 2016; WHO, 2007). Notwithstanding the advantages, the use of AmB has some limitations: acute side effects, such as nausea, fever and chills; severe nephrotoxicity and hepatotoxicity; and its poor solubility in aqueous solution (Charvalos *et al.*, 2006; Laniado-Laborin & Cabrales-Vargas, 2009; Mendonca *et al.*, 2018). To overcome these issues, new strategies using AmB have been developed. The modification of the AMB molecule or its physical state and the use of drug delivery system (liposomal formulations, micellar dispersions, among others) have been the cornerstones to improve the therapeutic efficacy and to reduce the toxicity of AMB, even at high doses (Charvalos *et al.*, 2006; Chattopadhyay & Jafurulla, 2011; Laniado-Laborin & Cabrales-Vargas, 2009). Deoxycholate-solubilized AmB (Fungizone®) is a micellar dispersion that has been considered, for many years, the most effective and widely used drug for antifungal therapy. Although, Fungizone® is associated with severe toxic side effects, namely nephrotoxicity and renal failure. As a consequence of that, this micellar dispersion exhibits a narrow therapeutic index, hence some of its clinical limitations (Charvalos *et al.*, 2006; Serafim *et al.*, 2016). The previous stated issues motivated the development of lipid-based AmB formulations, such as AmBisome®. This liposomal formulation displays a more fitting size, allowing better penetration in the tissues and retention in the organs of interest. AmBisome® also has reduced toxicity to mammalian cells, due to the presence of cholesterol in its design, since it allows a decrease in the interaction between AmB and the host cell membrane. The rates of disease remission using AmBisome® go over 95%, but its means of administration (continuous intravenous injection) and high cost continue to

hamper its use, with the latter making it inaccessible to the low-income populations of developing countries (Charvalos *et al.*, 2006; Ehrenfreund-Kleinman *et al.*, 2002; Stone *et al.*, 2016; Sundar *et al.*, 2007).

Table 2 comprises the currently used drugs in leishmaniasis treatment, its efficacy rates, advantages, limitations and cost.

Table 2- Overview of the currently available anti-leishmanial drugs: efficacy, advantages, limitations and cost. Adapted from de Menezes *et al. (2015)* and O. P. Singh *et al.* (2016)

Drug	Efficacy	Advantages	Limitations	Cost
Pentavalent antimonials	35–95 % (depending on the geographical area)	Low cost, high drug amount in the infection site, easy availability	Drug resistance, cardiotoxicity, prolonged and painful treatment	50–198$
Pentamidine	35–96 % (depending on the *Leishmania* species)	Low doses are required, Effective in combined therapy	Severe side effects (diabetes mellitus or myocarditis), high cost	ND (Non-Described)
Paromomycin	94 % (India), 46–85 % (Africa)	Low cost, Bactericidal activity	Severe nephrotoxicity and ototoxicity, pain in the injection site	10–15$
Miltefosine	94% (India); 60%–93% (Africa)	Good oral absorption, Effectiveness in CL and VL, Domiciliary treatment	Long treatment period, high possibility of parasite resistances, teratogenic potential	70–150$
AmB Sodium deoxycholate micelle system (Fungizone®)	>98%	High efficacy, Low cost	Narrow therapeutic index, nephrotoxicity and renal failure	~ 21–100$
Liposomal AmB (AmBisome®)	>98%	High efficacy, Reduced toxicity	High cost, Continuous intravenous injection to be effective	280–3000$

1.2.1.6 Combined therapy

The combination of multiple drugs to treat leishmaniasis has also displayed a relevant role in the struggle to control this disease. Multidrug therapy aims to: increase the efficacy rate, promote a higher patient compliance by reducing treatment duration, decrease the therapy cost and finally, delay the emergence of parasite resistance (Ghorbani & Farhoudi, 2018; O. P. Singh *et al.*, 2016; van Griensven *et al.*, 2010). Dorlo *et al.* (2012) have shown that the association of miltefosine with liposomal AmB could result in decreased treatment duration, while maintaining the high efficacy of the latter. In order to be successful, the drugs used in these type of procedures should have a synergetic effect, with one having strong and immediate effect and the other displaying a retarded action, to ensure that all the parasite burden is removed (Dorlo *et al.*, 2012; O. P. Singh *et al.*, 2016). The downside to this type of therapy is the existence of limited data and low reproducibility of effective results using multidrug therapies (de Menezes *et al.*, 2015; Ghorbani & Farhoudi, 2018; van Griensven *et al.*, 2010).

1.2.2 Vaccines

Vaccines are perceived as the cornerstone therapy to ensure that this disease is preventable or eliminated (Murray *et al.*, 2005; Vijayakumar & Das, 2018). Ideally, an effective vaccine should ensure a long-lasting immunity to the host and its mechanism of action should be based in a well-adjusted T_H1- and T_H2-mediated immune response (Gillespie *et al.*, 2016).

The development of vaccines has been limited by the lack of knowledge of the immune response and its effects on parasite growth (Kedzierski, 2010; O. P. Singh *et al.*, 2016; O. P. Singh & Sundar, 2014). So far, three different vaccine types are available: first-, second- and third-generation vaccines. First-generation vaccines are made of dead parasites and have emerged, in the past, as an alternative to leishmanization, but display poor efficacy in clinical trials and its regularization is somewhat troublesome. Second-generation vaccines are based on genetically modified

parasites or viruses expressing leishmanial antigens. Similarly to the first-generation, these vaccines have failed to show efficiency although presenting protection in animal models. Third-generation vaccines, also named as DNA vaccines, have a lower cost of production and higher stability in relation to its predecessors. However, DNA vaccines' potential remains inconclusive due to the lack of clinical data (Ghorbani & Farhoudi, 2018; Kedzierski, 2010).

1.2.3   Drug delivery systems

As previously stated, the available chemotherapies are far from being the ideal solution to treat leishmaniasis. Although some of these are highly effective, each one has a plethora of obstacles limiting its widespread use, such as high costs, acute side effects or high associated toxicity (Akbari *et al.*, 2017; de Souza *et al.*, 2018). *Leishmania spp.* are intracellular obligatory parasites and its main target are the host phagocytic cells. When internalized by these cells, *Leishmania* parasites have the capacity to survive and replicate, evading the host' immune response. The location of the parasites, inside the phagolysosome, constitutes a protective shield against some of the anti-leishmanial drugs (Kapil *et al.*, 2018; Naderer & McConville, 2008; Panaro *et al.*, 1995; D. M. Walker *et al.*, 2014). Drug delivery systems are expected to abbreviate this problem. Different drug carriers, including liposomes, emulsions or nanoparticles, have been developed and present further relevant features, such as higher drug bioavailability and selective targeting of phagocytic cells, alongside with less toxicity to uninfected cells (Akbari *et al.*, 2017; de Souza *et al.*, 2018). Moreover, these systems are crucial to increase the aqueous solubility of some anti-leishmanial drugs, since most of them are poorly water-soluble, a characteristic that highly hinders its efficiency (de Souza *et al.*, 2018). Finally, due to its size, nanosized drug delivery systems are easily taken up by phagocytes, allowing an increase of the drug concentration in the infected site, more specifically in the phagolysosome (Akbari *et al.*, 2017; Gutierrez *et al.*, 2016; Kreuter, 1991).

Over the last half-century, liposomes have been widely explored for clinical applications in cancer treatment, fungal infections or inflammatory diseases. Liposomes most interesting feature is probably their capacity to encapsulate hydrophilic or hydrophobic drugs, enhancing the drugs therapeutic index. Ambisome®, above described, is the only FDA approved liposomal formulation to treat VL. Due to its small size (e.g., ≈100 nm), Ambisome® has the capacity to remain longer periods in circulation, in the blood, while maintain a stable form. Compared with the free drug, this formulation is also capable of liberating higher drug levels in the lesion site without prompting increased toxic effects (Bulbake *et al.*, 2017; de Souza *et al.*, 2018).

Emulsions, lipid-based drug carriers, have also appeared as an important strategy to treat this parasitic disease. With the possibility of being orally administrated, these formulations have the capacity to disseminate the drug to phagocytes in the liver, bone marrow or lymph nodes. A lipid-based AmB formulation demonstrated ability to enhance the drug' oral absorption in animal models (de Souza *et al.*, 2018; Ibrahim *et al.*, 2013). Nevertheless, this kind of therapeutic systems is poorly explored in the leishmaniasis field and little to no data on its toxicity is available (Mohamed-Ahmed *et al.*, 2012).

Polymeric nanoparticles comprise a relevant class of drug carriers, since these systems have the ability to bind drugs by dissolution, adsorption or encapsulation. Up to now, AmB polymeric-based delivery systems, used in the treatment of leishmaniasis, haven been mostly made of poly lactic-co-glycolic acid (PLGA) or Polyethylene glycol (PEG). Several studies have shown that these formulations have better biodistribution, higher therapeutic efficacy and more importantly, reduced toxicity, when compared with the free drug (de Carvalho *et al.*, 2013; Jain & Kumar, 2010; Kumar *et al.*, 2015; Radwan *et al.*, 2017; Souza *et al.*, 2015). Polysaccharides are a family of natural polymers that have been widely used as drug carriers (Seidi *et al.*, 2018; Zhang *et al.*, 2015). The main characteristics that make polysaccharides suitable to produce drug delivery systems are: biocompatibility, non-immunogenicity, biodegradability and low cost. More

importantly, the use of polysaccharides allows drug solubility and stability, prolonged circulation lifetime and activity, and reduced drug toxicity (Desbrieres *et al.*, 2018; Ickowicz *et al.*, 2014).

Arabinogalactan, dextran, cyclodextrin and pectin have been some of the chosen polysaccharides to formulate AmB-loaded systems (Ehrenfreund-Kleinman *et al.*, 2004; Golenser *et al.*, 1999; Kaneo *et al.*, 2014; Kothandaraman *et al.*, 2017). In order to produce these polysaccharide-AmB conjugates, the oxidation of the polysaccharide into a polyaldehyde is performed (Figure 5A and 5B).
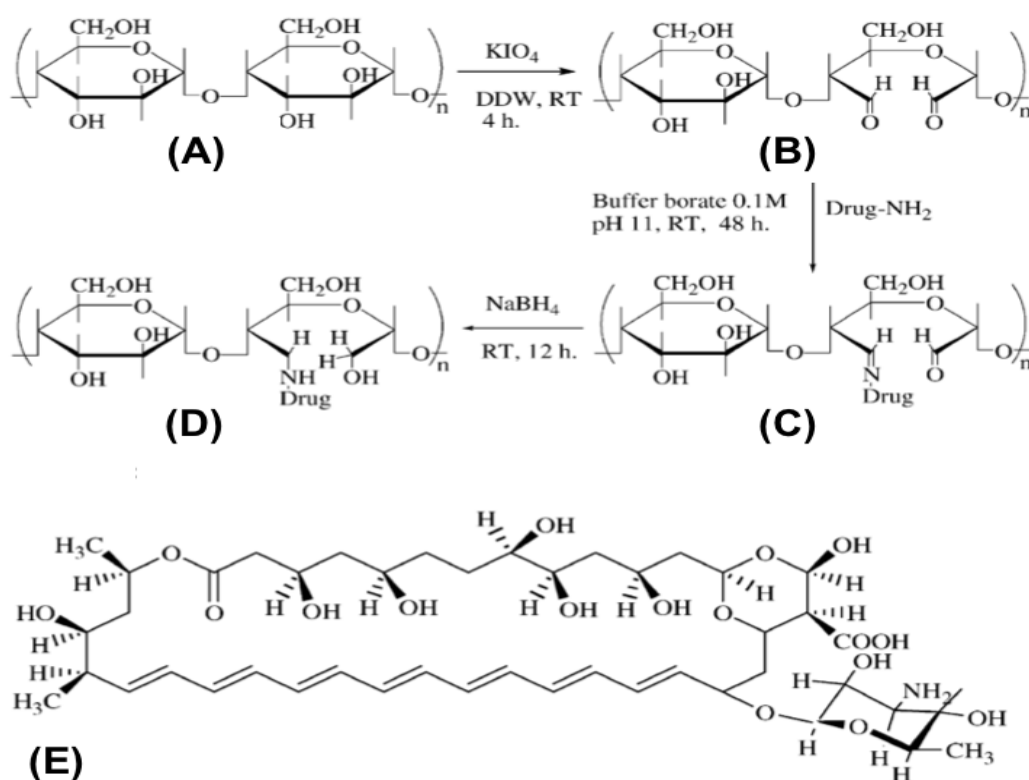
Figure 5- Schematic representation of the binding between oxidized Arabinogalactan and AmB via imine or amine conjugates: (A) Arabinogalactan, (B) oxidized Arabinogalactan, (C) Arabinogalactan-AmB imine conjugate, (D) Arabinogalactan-AmB amine conjugate and (E) AmB. Adapted from Ehrenfreund-Kleinman *et al.* (2002).

Afterwards, the binding between AmB and the oxidized polysaccharide occurs, according to those authors, through a Schiff base (reaction between the AmB's amine and the aldehyde of the reducing sugars in the polysaccharide), yielding an imine conjugate (Figure 5C). Moreover, some of these polysaccharide-AmB conjugates further require a reduction step to

form a more stable amine form (Figure 5D) (Ehrenfreund-Kleinman *et al.,* 2002; Kothandaraman *et al.,* 2017; Sokolsky-Papkov *et al.,* 2006)

These formulations have improved the solubility of AmB, resulting in higher therapeutic efficacy when compared to the free drug or other strategies (Ehrenfreund-Kleinman *et al.,* 2004; Golenser *et al.,* 1999; Kaneo *et al.,* 2014; Kothandaraman *et al.,* 2017).

1.2.3.1 Dextrin as a polysaccharide-based drug delivery system

Dextrin is a α-1,4 poly(glucose) oligomer, being obtained by partial hydrolysis, in enzymatic or acidic conditions, of glycogen or starch. Accumulation problems in tissues are prevented, even following repeated administrations, since dextrin has a low molecular weight (< 40 kDa) and its *in vivo* degradability is assured by amylases. Other physicochemical characteristics make this group of carbohydrates particularly interesting for drug carrier purposes, namely, their high biocompatibility, non-immunogenicity, water-solubility and biodegradability *in vivo*. Dextrin based formulations could also circumvent the economic problems associated with liposomal formulations, since this material is of low cost (Carvalho *et al.,* 2007; Hreczuk-Hirst *et al.,* 2001; Moreira *et al.,* 2010; Silva *et al.,* 2014). Although dextrin is already well-established in the biomedical field as wound dressing vehicle, peritoneal dialysis solution and carrier for antitumoral drugs, it is still rather unexplored in the biomaterials field (Debusk V, 2006; Kerr *et al.,* 1996; Peers & Gokal, 1998). Furthermore, Goncalves *et al.* (2010) have shown that Dextrin-based nanoparticles may have interesting potential for targeted intracellular delivery of drugs, especially to phagocytic cells, due to its effective internalization.

2. Aims

Leishmaniasis control and elimination remains troublesome, despite all the scientific community' efforts. Amphotericin B (AmB) is currently a gold standard drug recommended by the World Health Organization but presents itself as a highly water insoluble and toxic compound with reduced stability. To overcome these issues, several drug delivery systems have been developed, such as sodium deoxycholate micellar dispersions (Fungizone®) or liposomal formulations (AmBisome®). Notwithstanding its high effectivity, these formulations still raise some concerns. It is, therefore, of urgent need the development of alternative effective strategies.

More recently, polysaccharide-based formulations (covalent conjugates) for the delivery of AmB have been worthy of interest, since they have been proving to meet such demands. These drug delivery systems allowed drug solubility and stability, prolonged circulation lifetime and activity, reduction of drug toxicity and targeted delivery. Yet, in some cases oxidation steps (Farber *et al.*, 2011; Golenser *et al.*, 1999; Kothandaraman *et al.*, 2017; Nishi *et al.*, 2007; Ravichandran & Jayakrishnan, 2018; Sokolsky-Papkov *et al.*, 2006) are required during the production, potentially increasing the cost, toxicity and process complexity.

Most of the polysaccharide-based AmB formulations reported in the literature are believed to arise from a reaction between the AmB's amine and the aldehyde of the oxidized polysaccharide, forming a Schiff-base (Farber *et al.*, 2011; Golenser *et al.*, 1999; Kothandaraman *et al.*, 2017; Nishi *et al.*, 2007; Ravichandran & Jayakrishnan, 2018; Sokolsky-Papkov *et al.*, 2006). However, previous studies (unpublished data) done by our research group suggest that AmB interacts with polysaccharides forming stable micelles without any covalent bond. Indeed, the exploratory work performed in our group suggest that under the conditions reported in the literature, covalent conjugates are not formed and therefore these formulations arise from a self-assembling process involving weaker forces.

We hypothesize that dextrin may be an interesting polysaccharide for the development of an AmB delivery system, due to its intrinsic features (described in section 1.3.3.1). Herein, we propose the development of a Dextrin-Amphotericin B (Dex-AmB) formulation to improve the solubilization and delivery of AmB to *Leishmania* infected cells, while reducing its toxicity. In order to do so, the work was divided in the following steps:

a) Production of a Dex-AmB formulation through non-specific interactions between the two molecules;

b) Development of an HPLC method to quantify AmB in the formulation, using mass detector (MS) and ultra-violet detector (UV);

c) Biophysical characterization of the produced formulation;

d) Evaluation of the *in vitro* biocompatibility of Dex-AmB formulation towards bone marrow-derived macrophages (BMMΦ) and evaluation of its *in vitro* efficacy against *Leishmania* axenic promastigotes and intramacrophagic amastigotes;

3. Materials and Methods

3.1 Materials

Amphotericin B (AmB) powder from *Streptomyces sp.,* Sodium tetraborate decahydrate, Potassium periodate, Sodium Borohydride, Diethylene glycol (DEG), Potassium hydrogenphthalate (KHP), Hydroxylamine, Methyl Orange, Phenolphthalein, Resazurin Sodium salt, 4',6-diamidino-2-phenylindole (DAPI), Triton X-100, Paraformaldehyde, α-Amylase (from human saliva), Schneider's Insect medium were purchased from Sigma-Aldrich (St. Louis, MO, USA). Dextrin Tackidex® (medical grade dextrin from potato starch) with a degree of polymerization (DP) of 16 glucose residues and a branching degree of 9 % (Silva *et al.,* 2014) was a gift from Roquette (Lestrem, France). Dulbecco's Modified Eagle Medium (DMEM), fetal bovine serum (FBS), L-glutamine and penicillin-streptomycin were obtained from Merck Millipore (Burlington, Massachusetts, USA). Roswell Park Memorial Institute (RPMI) 1640 Glutamax was purchased from Gibco (Massachusetts, USA). Dimethyl sulfoxide (DMSO) was acquired from Fisher Scientific (New Hampshire, USA). Dialysis tubing with a molecular weight cut-off of 1000 Da was obtained from Orange Scientific (Braine-l'Alleud, Belgium). High-content screening (HCS) CellMask™ Deep Red stain was acquired from Invitrogen (Carlsbad, California, USA). Sodium hydroxide, Hydrochloric acid (HCl), Acetonitrile and Formic acid (both being analytical grade or equivalent) were purchased from Fisher Scientific (Hampton, New Hampshire, USA).

3.2 Production of Dextrin-Amphotericin B formulation

3.2.1 Preparation of Borate Buffer 0.1 M pH 11

A solution of 0.1 M sodium tetraborate decahydrate was prepared. This solution was heated under continuous stirring to achieve complete dissolution of the reagent. Finally, 4 M of NaOH was added to adjust the pH to 11.

3.2.2   Pre-dialysis of Dextrin

The dextrin (e.g. dextrin Tackidex) used presents a large size distribution of around 4.5 kDa, as shown by Silva *et al.* (2014). Therefore, a pre-dialysis of dextrin using a low molecular weight cut-off (1000 Da) membrane was performed. Briefly, 1.5 g of Dextrin Tackidex was dissolved in distilled water (dH$_2$O), at a concentration of 10 mg/mL. Then, this solution was dialyzed against 5 L of dH$_2$O, with 2 water exchanges per day, for 72 h. A dialysis membrane with a low molecular weight cut-off (1000 Da) was used. After that, the material was dried in a Freeze-Dryer (Coolsafe 100-9 Pro, Labogene, Lillerød, Dinamarca). This pre-dialysis was carried out to remove the smaller dextrin molecules, ensuring that AmB would not be lost in the following dialysis step of the synthesis process.

Of note, from this moment forward we will refer to dextrin as the dialyzed and lyophilized form of the compound.

3.2.3   Dextrin-Amphotericin B formulation synthesis

AmB is an amphiphilic molecule with poor solubility in water and in many organic solvents. When in aqueous solution, at a physiological pH, AmB tends to form high-molecular-weight aggregates. To circumvent this problem, borate buffer may be used to increase AmB solubility, since the borate ions complexes the AmB diols (at an alkaline pH), making it available for self-assembling/conjugation with Dextrin (Ehrenfreund-Kleinman *et al.*, 2002; Ernst *et al.*, 1981; Gershkovich *et al.*, 2009; Strauss & Kral, 1982). Ehrenfreund-Kleinman *et al.* (2002) showed that borate buffer promotes higher formulation overall yields (%) when compared to other buffers (e.g. carbonate or phosphate). Thus, in this work, the borate buffer with pH of 11, was used as a reaction media in the development of Dex-AmB formulations.

Four formulations were prepared: 32 mg of dextrin were dissolved in 3.2 mL of 0.1 M Borate buffer, pH 11. Then, 8 mg of AmB, corresponding to 8.672 x10^{-6} mol, were added to each solution. The resulting solutions were maintained under magnetic stirring for 48 h, at 4 °C, protected from light. The pH was frequently monitored and adjusted to 11 with NaOH. All samples

were dialyzed (to remove the alkaline buffer), using a 1000 Da cut-off membrane, against 2 L of dH$_2$O, in a light-protected container. During this process, the number of dH$_2$O exchanges were controlled in order to obtain a final pH of approximately 6. After this step, all samples were frozen at - 80 °C and freeze-dried to obtain yellow-orange Dex-AmB formulation. The formulations were weighted and stored in falcons at 4°C, until use (Figure 6).

A scale-up assay increasing the amounts used by 10-fold was also performed, where dextrin and AmB mass as well as Borate buffer volume were increase proportionally. The dialysis step was performed against 5 L of dH$_2$O. From this point forward, Dextrin-Ampohotericin B formulation will be referred to as Dex-AmB formulation, unless otherwise stated.
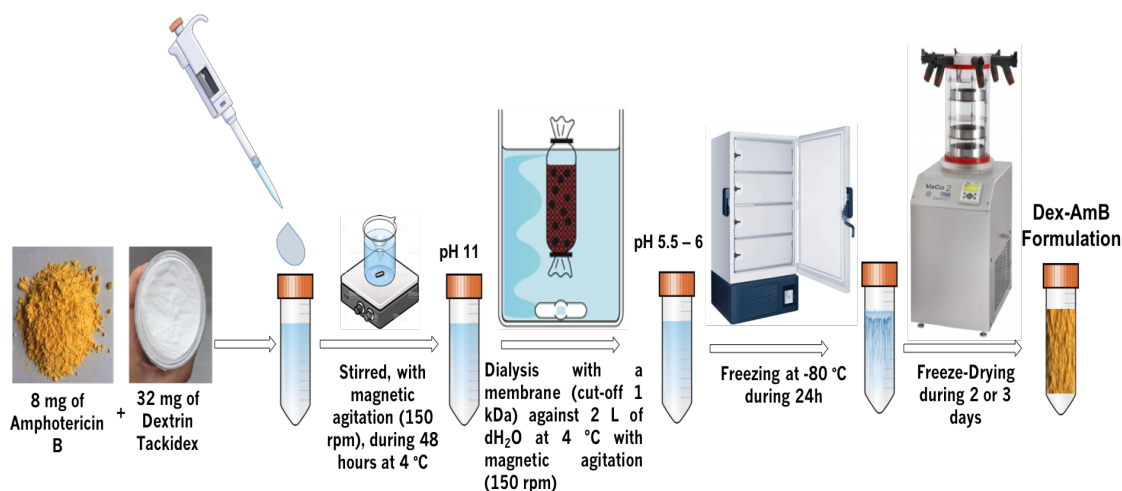
Figure 6- Schematic representation of the production process of the Dex-AmB formulation, at a small scale.

3.2.4   Formulation sterilization

Stock solutions of Dex-AmB formulation were filtered using a 0.22 pore size sterile filter (Tecnocroma, Caldas da Rainha, Portugal), to ensure sterility. Alternatively, the Dex-AmB formulation was sterilized in an Ethylene Oxide (EtO) chamber. This sterilization process was performed for 15 h, at 53 °C ± 1 °C.

3.3 Production of Dextrin-Amphotericin B Imine and Amine Conjugates

3.3.1 Dextrin Oxidation

Oxidized dextrin was obtained through an adaptation of the Sokolsky-Papkov *et al.* (2006) protocol. Briefly, 1 g of Dextrin was dissolved in Milli-Q water and then, 0.8625 g of Potassium Periodate were added. This aqueous solution was magnetically stirred for 6 h, protected from light. Then, 90 μL of diethylene glycol (DEG) were added and the solution was stirred for further 30 min in order to remove unreacted periodate ions. The resulting solution was dialyzed against 5 L of dH$_2$0, for 48 h at 4 °C, using a 1000 Da cut-off membrane. Four changes of water were made. Finally, the material was freeze-dried. From this point forward, oxidized Dextrin conjugate will be referred to as OxDex, unless otherwise stated.

3.3.2 Degree of Oxidation (DO %) by Hydroxylamine Hydrochloride Method

Hydroxylamine Hydrochloride titration was performed to estimate the degree of oxidation (DO %) of OxDex, using a modified protocol described by Zhao & Heindel (1991). Due to the tendency of NaOH to absorb CO$_2$ from the atmosphere, NaOH was first titrated with KHP prior to its use to titrate OxDex. Briefly, a 0.1 M NaOH solution was prepared and 33.25 mg of KHP were dissolved in 10 mL of dH$_2$O with Phenolphthalein (0.5 % w/v). The NaOH solution was titrated against KHP, until a stable pink color was reached. At the equivalence point, the added volume of NaOH and KHP's number of moles were used to calculate the molar concentration of NaOH, using equations 4, 5 and 6:

$$n_{KHP} = \frac{m_{KHP}}{M_{KHP}}$$

(Equation 4)

$$n_{KHP} = n_{NaOH} \text{ (at the stoichiometric point)}$$

(Equation 5)

$$M_{NaOH} = \frac{n_{NaOH}}{V_{NaOH}}$$

(Equation 6)

Where V_{NaOH} represents the volume of NaOH to reach the stoichiometric point.

Therefore, to prepare a 0.25 N Hydroxylamine Hydrochloride solution, 17.5 g of this reagent were dissolved in dH_2O and 6 mL of methyl orange reagent (0,05 % v/v) was added. Using NaOH, the pH of the solution was adjusted to 4. Afterwards, 20 mg of both OxDex and dextrin (to be used as a positive control) were dissolved in the hydroxylamine hydrochloride solution, for 3 h, under magnetic stirring. Both solutions were titrated with 0.1 M NaOH, until the equivalence point was reached (i.e., solution goes from a red to a light-yellow color). The degree of oxidation (DO %) of OxDex was calculated using the following equations:

$$n_{OxDEX} = \frac{m_{OxDEX}}{Mw}$$

(Equation 7)

$$n_{DEX} = \frac{m_{DEX}}{Mw}$$

(Equation 8)

$$n_{NaOH} = \frac{M_{NaOH}}{V_{NaOH}}$$

(Equation 9)

$$Degree\ of\ Oxidation\ (D.O\ \%) = \left(\frac{n_{NaOH}}{n_{OxDEX}} \times 100\right) - \left(\frac{n_{NaOH}}{n_{DEX}} \times 100\right)$$

(Equation 10)

Where V_{NaOH} represents the volume of NaOH to reach the stoichiometric point; n_{OxDEX} and n_{DEX} were calculated using the molecular weight (Mw) of a single glucose monomer minus a water molecule (162 g/mol) that is lost during the condensation reaction to form the glycosidic bond between glucose monomers.

3.3.3   Conjugation Step

An adapted protocol of Sokolsky-Papkov *et al.* (2006), was used to conjugate OxDex to AmB. Dextrin-Amphotericin B imine conjugate was

obtained by adding 32 mg of dextrin to 3.2 mL of 0.1 M borate buffer (pH 11). When the dissolution was completed, 8 mg of AmB were added and the solution was stirred for 48 h, at room temperature and light-protected. The dialysis and freeze-drying conditions of this conjugate were the same as the one's described for the Dex-Amb conjugate.

The Dextrin-Amphotericin B amine conjugate was produced by adding 32 mg of Sodium Borohydride to the solution prepared as stated previously. This new solution was further stirred overnight. In the end, it was dialyzed and freeze-dried as described above.

From this point forward, Dextrin-Amphotericin B imine and amine conjugates will be referred, respectively, to as ImDex-AmB conjugate and AmDex-AmB conjugate, unless otherwise stated.

3.4 HPLC-UV and Mass Spectroscopy Analysis

3.4.1 Instrumentation and HPLC conditions

AmB was quantified using a Finnigan LXQ High Performance Liquid Chromatography (HPLC) system (ThermoElectron Corporation, Massachusetts, EUA) equipped with a Surveyor Autosampler. The analytical column was a Kinetex® C18 100 Å 100 mm x 4.6 mm, with a 2.6 µm particle size, from Phenomenex (Torrance, CA). Two types of detectors were used: a photodiode array (PDA) wavelength detector (Waters 2998) and an ion trap Mass Spectrometer (MS) equipped with an ElectroSpray Ionization (ESI) source. All spectral data were acquired and analyzed using Xcalibur Chromatography Software (Thermo Fisher Scientific, Massachusetts, USA). The source dependent parameters such as Sheath Gas flow rate, Auxiliar Gas flow rate, Sweep Gas flow rate, Tube Lens, Capillar Voltage, Capillar Temperature and Spray Voltage were optimized to values of 50 arb, 10 arb, 10 arb, 115 Volts, 29 Volts, 250 °C and 5000 Volts, respectively.

The mobile phase was composed of two solvents previously filtered and degassed: (A) Milli-Q Water with 0.1 % (v/v) formic acid and (B) Acetonitrile with 0.1 % (v/v) formic acid. Gradient elution conditions were established and are shown in Table 3. The method run time was 20 minutes,

with a flow rate of 0.3 mL/min and an injection volume of 25 μL. Analysis was performed at a temperature of 25 °C.

In order to quantify the amount of Amphotericin B in the formulation, the two channels of the UV detector were set as follows: channel A at 387 nm and channel B at 408 nm. For the Mass Spectrometer, analysis was made using a Selected Ion Monitoring (SIM) Mode with scan ranges from 923 to 925 m/z, and the instrument was operated in Positive Ionization Mode (M + H$^+$).

Table 3- Gradient elution program

Time (Minutes)	Mobile Phase A[a] (%)	Mobile Phase B[b] (%)	Flow Rate (mL/min)
0.00	50	50	
8.00	10	90	
16.00	50	50	0.3
20.00	50	50	

[a] Milli-Q Water with 0.1% (v/v) formic acid; [b] Acetonitrile with 0.1% (v/v) formic acid

3.4.2 Preparation of Amphotericin B and Dextrin-Amphotericin B formulation solutions

Stock standard solutions of AmB and Dex-AmB, at a final concentration of 150 μg/mL and 3000 μg/mL, respectively, were prepared by dissolving each material in acetonitrile:milli-Q water:formic acid (39.22:58.33:2.45 % (v/v)), under mild stirring and protected from light, during 2 h at 4 °C. Subsequently, for the calibration curve, different solutions of AmB at 2, 5, 10, 20, 60, 80 and 120 μg/mL were prepared from the stock standard solution using acetronitrile:milli-Q water (39.22:60.78 % (v/v)). Similarly, for the DeX-AmB formulation, solutions of 100 μg/mL were prepared using the above mentioned solvent. Prior to injection, standards and samples were filtered using a 0.22 pore size Nylon filter (Tecnocroma, Caldas da Rainha, Portugal).

Linear calibration curves relating AmB concentration and peak area were made. Finally, the quantity of AmB in the Dex-AmB formulation was

obtained by interpolation of peak area, for each sample, in the calibration curve.

3.5 Dextrin-Amphotericin B formulation characterization

3.5.1 Average Size and Polydispersion Index by DLS

The hydrodynamic diameter and Polydispersion index (PDI) of the formulations were assessed by Dynamic Light Scattering (DLS).

The Dex-AmB formulation and dextrin were dissolved in distilled water (dH$_2$0), at a formulation concentration of 1 mg/mL. Then, prior to the analysis, the samples were diluted to reach a final concentration of 50 μM (in AmB). A part of the samples was filtered through a 0.22 μm PES syringe filter (Tecnocroma, Caldas da Rainha, Portugal), as they would if added to the cells. Prior to the analysis, the solutions were stirred, in a rotary mixer (Orange Scientific, Braine-l'Alleud, Belgium), for 48 h at 4°C.

All the samples were placed in polystyrene cuvette for size distribution and analyzed using a ZetaSizer Nano ZS (Malvern, Worcestershire, UK), with a He-Ne gas laser (633 nm), a folded capillary cell and a detector angle of 173°.

For each sample, PDI and z-average diameter, corresponding to the mean hydrodynamic diameter, were evaluated after 5 repeated measurements. The Dispersion Technology Software version 6.01, from Malvern (Worcestershire, UK), was used to collect and analyze the data.

3.5.2 Particle Concentration and Size by NTA

The particle size and concentration of the formulations were assessed by Nanoparticle tracking analysis (NTA).

Dex-AmB formulation and dextrin were dissolved, for 48 h, in dH$_2$0, at a formulation concentration of 1 mg/mL. Then, prior to the analysis, the sample was diluted to reach a final concentration of 50 μM (in AmB). A part of the samples was filtered through a 0.22 μm PES syringe filter (Tecnocroma, Caldas da Rainha, Portugal), as they would if added to the cells. Using a syringe (BD Discardit II, New Jersey, USA), the samples were

placed in the chamber sample. The samples were analyzed for 60 s, using manual shutter and gain adjustments. The measurements were performed in a NanoSight NS 500 (Malvern, Worcestershire, UK) with a 640 nm laser was used.

For each sample, the particle size and concentration were obtained by performing 3 repeated measurements. All the assays were performed at room temperature and the NTA 2.3 Build 0017 software was used to collect the data.

3.5.3 Morphology

The morphology of the Dex-AmB formulation in solution was confirmed by cryo-SEM analysis. The SEM / EDS exam was performed using a High-Resolution Scanning Electron Microscope with X-Ray Microanalysis and CryoSEM, as detailed ahead.

Dex-AmB formulation was dispersed in dH_2O at a concentration of 2 mg/mL and rapidly cooled plunging it into sub-cooled nitrogen. The sample was transferred under vacuum to the cryo stage of the preparation chamber (Gatan, Alto 2500, UK). Then, the sample was fractured and sublimated for 120 seconds, at -90 °C, to remove the superficial ice layer and allow the Dex-AmB formulation to be exposed. Finally, the sample was sputter-coated with gold (Au) and palladium (Pd) for 45 s and transferred to the observation chamber of an electron microscope (SEM/EDS: JEOL JSM 6301F/Oxford Inca Energy 350). The observation was performed at -150 °C, 15 kV and a 12 mA current.

3.5.4 Recovery efficiency, Drug loading and Overall Yield

The drug recovery efficiency (RE %) was determined using the developed HPLC method, described in section 3. In order to assess the most accurate equipment for AmB quantification, two different HPLC detectors, namely mass (MS) and Ultra-Violet (UV), were used and the results compared.

To calculate the recovery efficiency (%), as well as the drug loading (% w/w) and the formulation production Overall Yield (%), the following equations were used, respectively:

$$AmB\ Recovery\ Efficiency\ (\%) = \frac{m_{AMB}}{m_{AMB\_initial}} \times 100$$

(Equation 1)

$$AmB\ Content\ (\%\ w/w) = \frac{m_{AMB}}{m_{DEX-AMB\_final}} \times 100$$

(Equation 2)

$$Overall\ Yield\ (\%) = \frac{m_{DEX-AMB_{final}}}{m_{DEX\_initial} + m_{AMB\_initial}} \times 100$$

(Equation 3)

where m_{AMB} is the AmB mass in the final formulation that was obtained via HPLC-MS or HPLC-UV (calculated for two wavelengths: 387 nm and 408 nm) and $m_{DEX-AMB}$ is the final mass of the produced formulation.

3.6 Cell and Parasite Bioassays

3.6.1   L929 Cell-conditioned media

In order to promote Bone marrow-derived macrophages (BMMΦ) differentiation, a growth factor is needed. Macrophage colony-stimulating factor (M-CSF), has been used to differentiate macrophages *in vitro* (Manzanero, 2012). L929 fibroblasts have the capacity to secret high amounts of M-CSF, so they are used to obtain this growth factor, at a low-price (Boltz-Nitulescu *et al.*, 1987; Stanley *et al.*, 1978). Considering that, it is possible to use the L929 Cell-conditioned media (LCCM) to differentiate bone marrow cells into macrophages. The latter was prepared based on a previous method, described by K. Z. Walker *et al.* (1986). Thus, L929 cells were grown in T75 Culture flasks at an initial density being of 5 x 10³ cells/mL, using 50 mL of RPMI complete medium (10 % FBS; 1 % Penicillin: Streptomycin). Cells were incubated in a humidified chamber (37 °C, 5 % CO_2), for 8 days. Afterwards, the culture medium was collected and centrifuged (300 g, 10 min). Finally, the supernatants were collected, filtered

through a 0.2 µm PES filter (Orange Scientific, Braine-l'Alleud, Belgium) and stored at -20 °C, until use.

3.6.2 Bone marrow-derived macrophages (BMMΦ) – Isolation and culture

BMMΦ used during this study were obtained from BALB/$_c$ mice, using a protocol adapted from Gomes *et al. (2008)*. Briefly, both the tibias and femurs of mice were collected, and the bone marrow cells were isolated by flushing the bones with DMEM medium. Then, the cell suspension was centrifuged (300 g, 10 min), with the supernatant being discarded. The cellular pellet was resuspended in DMEM supplemented with 1 % (v/v) Minimum Essential Medium Non-Essential (MEM) amino acids solution (Gibco, Massachusetts, USA), 10 % (v/v) inactivated fetal bovine serum (iFBS), 10 % (v/v) L929 cell conditioned medium (LCCM), 50 U/mL penicillin, 50 µg/mL streptomycin (complete differentiation media), placed in Petri dishes and incubated in a humidified chamber (37 °C, 5 % CO_2) for 24 h. After that period, non-adherent cells were collected, counted in a *Neubauer* chamber and plated in 96-well plates, at a density of 2.5 x 10^4 cells/well. These cells were incubated in a humidified incubator (37 °C, 5 % CO_2) for 10 days, with complete differentiation medium renewal on the 4th and 7th days.

3.6.3 Parasite cultures

Leishmania infantum promastigotes (MHOM/MA/67/ITMAP-263) and *Leishmania major* promastigotes (MRHO/IR/76/ER) were cultured in RPMI 1640 Glutamax supplemented with 10 % (v/v) iFBS, 50 U/mL penicillin, 50 µg/mL streptomycin (Gibco, Massachusetts, USA) and 20 mM HEPES pH 7.4 (Sigma-Aldrich, St. Louis, MO, USA). *Leishmania amazonensis* promastigotes (MHOM/BR/LTB0016) were cultured in Schneider's Insect medium supplemented with 10 % (v/v) iFBS, 100 U/mL penicillin, 100 µg/mL streptomycin, 5mM HEPES pH 7.4 and 5 µg/mL phenol-red (Sigma-Aldrich,

St. Louis, MO, USA) media. Parasite strains were maintained in culture at 26 °C and infectivity was ensured as described in Gomes-Alves *et al.* (2018).

Axenic amastigotes of *L. infantum* were obtained as described in Sereno & Lemesre (Sereno & Lemesre, 1997). The axenic amastigote culture was maintained in MAA (Medium for axenically grown amastigotes) medium supplemented with 20 % (v/v) iFBS, 2 mM Glutamax (Gibco, Massachusetts, USA), and 0.023 mM hemin (Sigma-Aldrich, St. Louis, MO, USA), at 37 °C, 5 % CO_2 and humidity.

3.6.4 Assessment of cytotoxicity to BMMΦ

In order to assess the cytotoxic potential of the Dex-AmB formulation and its individual components to BMMΦ, a standard resazurin assay was performed, as described by Vale-Costa *et al.* (2013). Briefly, BMMΦ cells obtained as above described, were submitted to increasing concentrations of the test compounds, previously dissolved in complete DMEM medium. After 24 h of incubation, at 37 °C with 5 % CO_2, 10 % (v/v) of a 2.5 mM resazurin solution was added to each well and the cells were incubated in the same conditions for another 2h. Then, fluorescence was measured (λ_{Ex} 560/λ_{Em} 590) in a SpectraMAX GeminiXS microplate reader (Molecular Devices LLC, CA, USA).

Viability results were calculated as a percentage (%) in relation to the control (i.e., BMMΦ cells in which no test compounds were added) and the 50 % cytotoxic concentration (CC_{50}) values were determined. All experiments were performed in duplicate.

3.6.5 Anti-leishmanial activity against axenic parasite cultures

Promastigotes were seeded in 96-well plates at 3 x 10^5 cells/well in RPMI complete medium or Schneider's Insect medium, according to the parasite species. Then, serial dilutions in the culture medium of free-AmB, Dex-AmB formulation and dextrin in the culture medium, were added to the respective wells. After 24 h incubation at 26 °C, parasite viability was assessed by resazurin assay (Vale-Costa *et al.*, 2013), using the same methodology as

described above. Of note, in some assays the Dex-AmB formulation was previously exposed to 77 U of α-amylase, for 2 h at 37 °C with 5 % CO_2, before being used in the *in vitro* assays.

Parasite viability and the IC_{50} values were calculated as referred to above. All experiments were performed in duplicate.

3.6.6 Anti-leishmanial activity against intramacrophagic *L. infantum* and *L. amazonensis* amastigotes

BMMΦ were seeded in 96-well plates, at a cell density of 1 x 10^5 cells/mL. Subsequently, BMMΦ were infected with *L. infantum* axenic amastigotes (3-days culture) or with *L. amazonensis* promastigotes (5-days culture) at a parasite:cell ratio of 10:1, for 3 h. After that, non-internalized parasites were removed by washing with complete DMEM medium the monolayers were incubated for further 24 h at 37 °C with 5 % CO_2.

Increasing concentrations of free-AmB, Dex-AmB and dextrin, diluted in DMEM complete medium, were added to the respective wells.

After 24 h incubation (37 °C; 5 % CO_2) with the compounds, the monolayers were fixed with paraformaldehyde (PFA) and stained with specific probes to assess the number of infected cells in each condition, as described by Gomes-Alves *et al.* (2018).

Anti-leishmanial activity results were expressed as an infection rate (%) (i.e., the quotient between the number of infected cells and the total number of cells, multiplied by 100), in relation to control, and the IC_{50} values were calculated.

3.7 Statistical Analysis

GraphPad Prism 7 software was used to analyze all date, unless otherwise stated.

4. Results and discussion

4.1 Production of Dextrin-Amphotericin B formulation

Four different batches of Dex-AmB formulation were produced, and, afterwards, a scale-up batch of 10 times larger. The overall yield (%) of the produced formulations is listed in Table 4.

Table 4- Overall yield (%) of Dex-AmB formulation recovery

Formulation	Overall Yield (%)
Dex-AmB Batch 1	66.6
Dex-AmB Batch 2	65.9
Dex-AmB Batch 3	68.3
Dex-AmB Batch 4	62.2
Dex-AmB Batch Scale-Up	71.1

Similar overall yields (%) between all the batches of Dex-AmB formulation were observed, indicating that the production process of the formulation is consistent regarding the final mass recovered. Thus, we decided to do a scale-up trial. The Dex-AmB formulation obtained at larger scale presented an overall yield (%) of 71.1 %, which is marginally higher than the ones obtained when producing at a smaller scale. All subsequent work was done using the larger Dex-AmB batch, in order to minimize the variability among different formulations.

Overall, the yield of Dex-AmB formulation production was slightly lower than that of other polysaccharide-based AmB formulations produced using the same reaction time (48 h). We hypothesized that this may be due to the low molecular weight of Dextrin Tackidex® (4.5 kDa) (Silva *et al.*, 2014), which is substantially lower than Galactomannan (54 kDa), Gum Arabic (250 kDa), Pectin (59 kDa), Arabinogalactan (12 kDa), Sodium alginate (51 kDa) and Dextran (40 kDa), and may be lost during dialysis. Thus, the material being lost in the process, perhaps in the dialysis step, is likely dextrin, being not clear from this result whether also AmB is being lost

to some extent. Still, the overall yield was considerably satisfactory (71.1 %) and superior to some values reported in the literature (Table 5).

Table 5- Reaction conditions and overall yield (%) of the scaled-up Dex-AmB formulation and other polysaccharide-based formulations reported in the literature

Reaction conditions	Formulation	Overall Yield (%)	References
RT of 48h, BB pH 11	Dex-AmB Batch Scale-Up	71.1	This work
RT of 48h, BB pH 11	Arabinologactan-AmB (Imine)	>90	(Ehrenfreund-Kleinman *et al.*, 2002)
RT of 48h, BB pH 11	Arabinologactan-AmB (Amine)	>90	
RT of 24h, BB pH 11	Sodium Alginate-AmB (Imine)	≈ 60	(Ravichandran & Jayakrishnan, 2018)
RT of 48h, BB pH 11	Galactomannan-AmB (Imine)	85	(Farber *et al.*, 2011)
RT of 48h, BB pH 11	Galactomannan-AmB (Amine)	80	
RT of 24h, BB pH 11	Pectin-AmB (Imine)	≈ 60	(Kothandaraman *et al.*, 2017)
RT of 48h, BB pH 11	Gum Arabic-AmB (Imine)	75	(Nishi *et al.*, 2007)
RT of 48h, BB pH 11	Gum Arabic-AmB (Amine)	80	
RT of 48h, BB pH 11	Dextran-AmB (Amine or Imine)	ND	(Sokolsky-Papkov *et al.*, 2006)

*Note: RT, reaction time; BB, borate buffer; ND, non-described.

4.2 Characterization of Dextrin-Amphotericin B formulation

4.2.1 AmB quantification - recovery efficiency and drug loading

While using spectrophotometry to assess the concentration of AmB, as it is widely used in the literature (Egger *et al.*, 2001; Eldem & Arican-Cellat, 2000; Rodrigues *et al.*, 2014; Wasan *et al.*, 2010), we noticed some lack of reproducibility and consistency. We thus concluded that a new methodology to quantify AmB could be desirable and useful. A method based on HPLC-MS was developed and used throughout this work.

The chromatography was performed using a gradient method as shown on table 3. As seen in Figure 7, the retention time of AmB was found to be at around three minutes, as detected by a tandem HPLC detector system, MS and UV, which was used for the AmB quantification. This retention time is far below what is already described in literature, where values of around 11 minutes (Espada *et al.*, 2008) or 25 minutes (Tan *et al.*, 2016) were reported, using respectively the following mobile phase/column: acetonitrile:acetic acid:water (52:4.3:43.7, v/v/v)/ BDS Hypersil C18 reverse-phase column and acetonitrile:acetic acid:water (48:4.3:47.7, v/v/v)/ BDS Hypersil C18 reverse-phase column. On the other hand, the obtained retention time was roughly equal to that reported by Qin *et al.* (2012). The chosen mobile phase appears to lead to a faster elution of AmB. Interestingly, although an AmB standard was analysed, two main peaks were detected, with retention times of around 2,8 and 3,4 mins, in addition to several smaller peaks. Indeed, the commercial AmB used has a purity of around 80%. Thus, a more polar solvent should be used in order to increase the retention time and allowing an improved resolution from contaminants.

The chromatogram and UV spectrum of an AmB standard, Dex-AmB formulation, dextrin and the mixture of solvents where the samples were prepared are shown in figure 8.
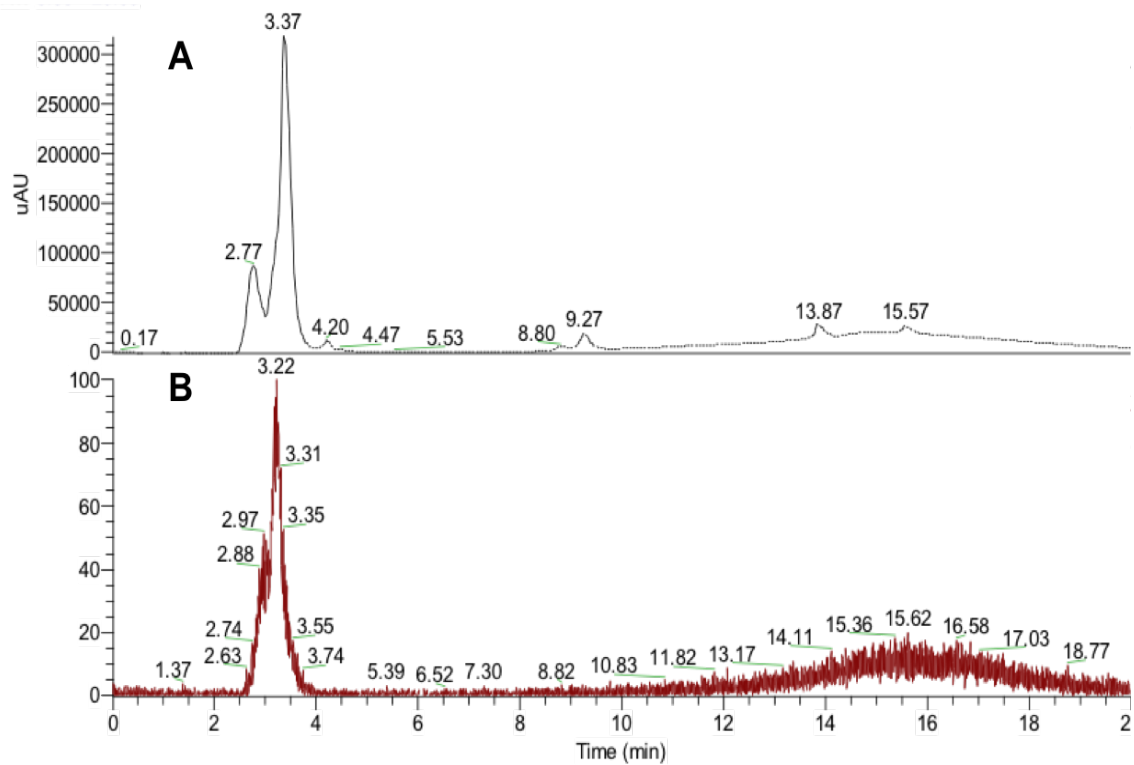
Figure 7- Representative chromatograms of AmB at 40 μg/mL using (A) HPLC-UV and (B) HPLC-MS.
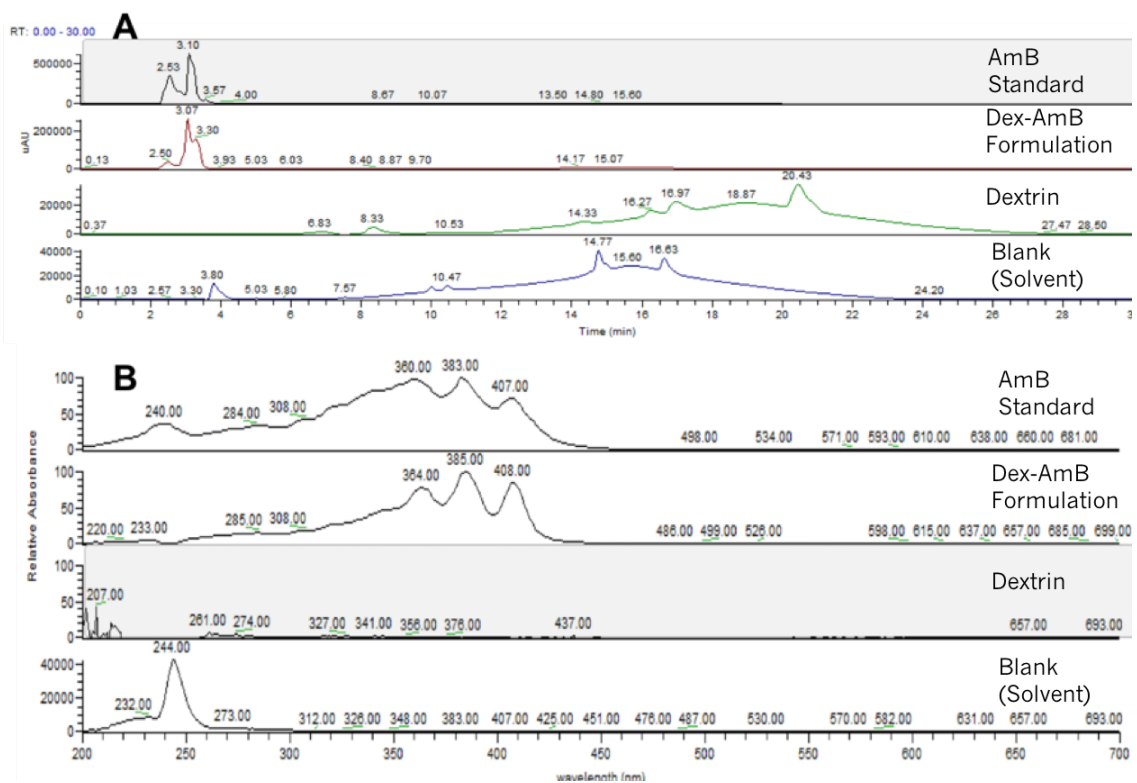
Figure 8- Representative (A) UV-chromatogram and (B) UV spectrum.

The UV spectrum of the AmB standard and Dex-AmB formulation presented the characteristic three main absorption peaks of AmB at roughly around 363, 382 and 407 nm (Casaccia *et al.*, 1991; Chang *et al.*, 2011). The chromatograms obtained with the controls (dextrin and solvent) using the UV detector and the respective spectra show that the dextrin and eluent used do not interfere in the UV detection of AmB (Figure 8).

The mass spectrum and MS-chromatograms of the AmB standard, Dex-AmB formulation and dextrin were detected using an HPLC-MS with mass scanning ranging from 0 to 2000 m/z (Figure 9). It was possible to identify the ion 923 m/z in both AmB standard and Dex-AmB formulation, at an elution time around 3 minutes as observed above, while other ions appeared in the mass spectrum of dextrin.
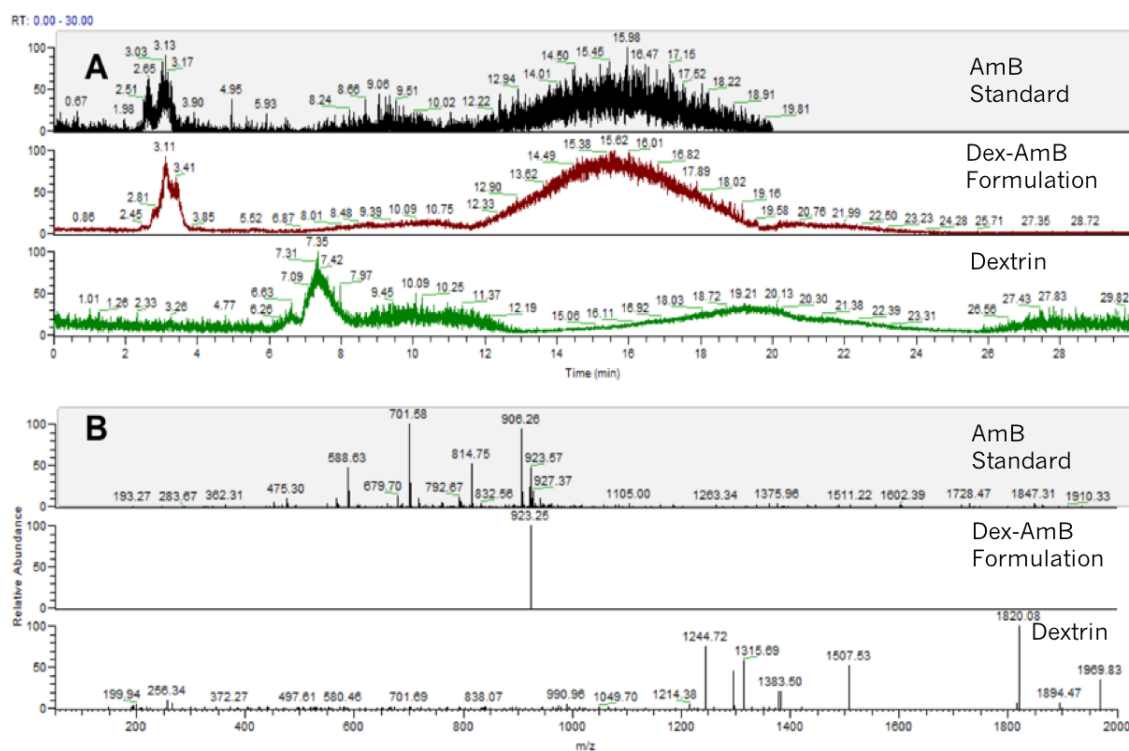
Figure 9- Representative (A) MS-chromatogram and (B) Mass spectrum.

To further complement the selectivity of the AmB detection in the HPLC analysis, we set the HPLC-MS at a Selected Ion Monitoring (SIM) Mode with scan ranges from 923 to 925 m/z (Positive Ionization Mode (M + H$^+$)),

since AmB has a molecular weight of 924.05 g/mol. The chromatograms are shown in Figure 10.
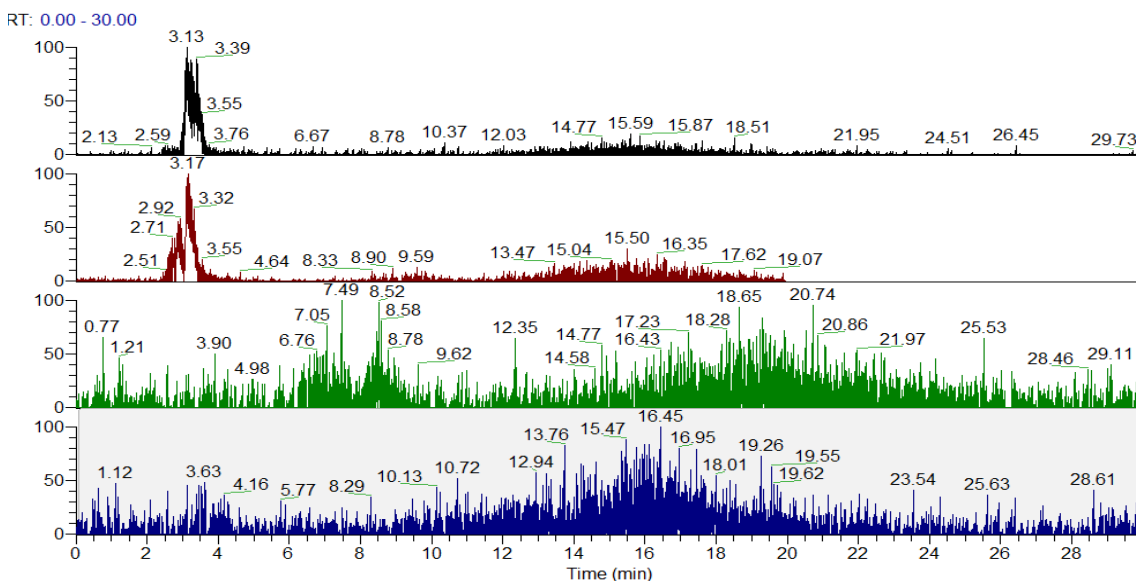
Figure 10- Representative MS-chromatograms of AmB standard (black peak), Dex-AmB formulation (red peak), dextrin (green peak) and blank (solvent) (blue peak).

It appears that, when using the HPLC-MS working in a Selected Ion Monitoring (SIM) Mode with scan ranges from 923 to 925 m/z, it is possible to selectively quantify AmB only, eliminating all signal arising from dextrin and the blank (solvent), as expected.

Hence, the quantification of AmB in the Dex-AmB formulation was carried out by using HPLC-UV (with the detector set at 387 and 408 nm) and HPLC-MS (working in a SIM Mode with scan ranges from 923 to 925 m/z).

The calibration curves obtained were linear in the ranges of 2-120 µg/mL of AmB, with r^2 values of 0.9992 (HPLC-UV 387 nm), 0.9991 (HPLC-UV 387 nm) and 0.9995 (HPLC-MS 923-925 m/z), which is above what is recommended for analytical methods ($r^2 > 0.999$) (Shabir, 2003). Finally, the AmB content (% w/w) and recovery efficiency (%) in the Dex-AmB formulation were determined, using the equations described in section 3.5.4. The results are expressed in Table 6.

Table 6- AmB content (% w/w) and AmB recovery efficiency (%) of Dex-AmB formulation obtained through the developed HPLC method, using Mass (MS) detector and UV detector (at 387 nm and 408 nm)

Formulation	AmB Content (% w/w)			AmB Recovery Efficiency (%)		
	MS	UV (387nm)	UV (408nm)	MS	UV (387nm)	UV (408nm)
Dex-AmB	37.62 ± 2.40	7.03 ± 0.45	6.13 ± 0.44	134 ± 8.57	31 ± 1.96	27 ± 1.97

The AmB content results obtained are quite different depending on whether they are estimated using the UV or the MS calibration curve. In literature reporting other polysaccharide-based AmB formulations, AmB contents (% w/w) of 34.4 % were described for a dextran-AmB conjugate (Sokolsky-Papkov *et al.*, 2006), 23 % for a arabinogalactan-AmB conjugate (Ehrenfreund-Kleinman *et al.*, 2002) and 20 % for a galactomannan-AmB conjugate (Farber *et al.*, 2011), when using HPLC-UV. None of these studies assessed the AmB content using HPLC-MS.

Also, the recovery efficiency of AmB (%) in the formulation was considerably lower when using the HPLC-UV method, as compared with the HPLC-MS method. For the latter, the AmB recovery efficiency was of 134 ± 8.57 %, while for HPLC-UV the values were of 31 ± 1.96 % (387 nm) and 27 ± 1.97 % (408 nm).

For both parameters, AmB content and recovery efficiency, the values obtained by HPLC-MS were roughly five times higher than the ones obtained by HPLC-UV. Thus, in order to assess which detection method (MS or UV) was the most accurate at quantifying AmB in the Dex-AmB formulation, a biological assay was performed. Two stock samples of Dex-AmB formulation (1 mg/mL of formulation) were prepared and then incubated with α-amylase for 2 h. This was made in order to rapidly degrade the dextrin within the formulation (Ferguson *et al.*, 2012). After the incubation period, a working solution of hydrolyzed Dex-AmB formulation (at a concentration of 5 μM of AmB) was prepared, based on the AmB content (% w/w) obtained either by HPLC-MS and HPLC-UV (for a wavelength of 387 nm). A working solution of

free-AmB (5 μM) was also prepared. Parasite viability was measured using a standard resazurin assay, after 24 h contact with the samples (Vale-Costa *et al.*, 2013).

For *L. amazonensis,* the dose-response curve of the formulation based on the MS quantification (Dex-AmB MS) was equal to the one obtained with free-AmB (Figure 11A).
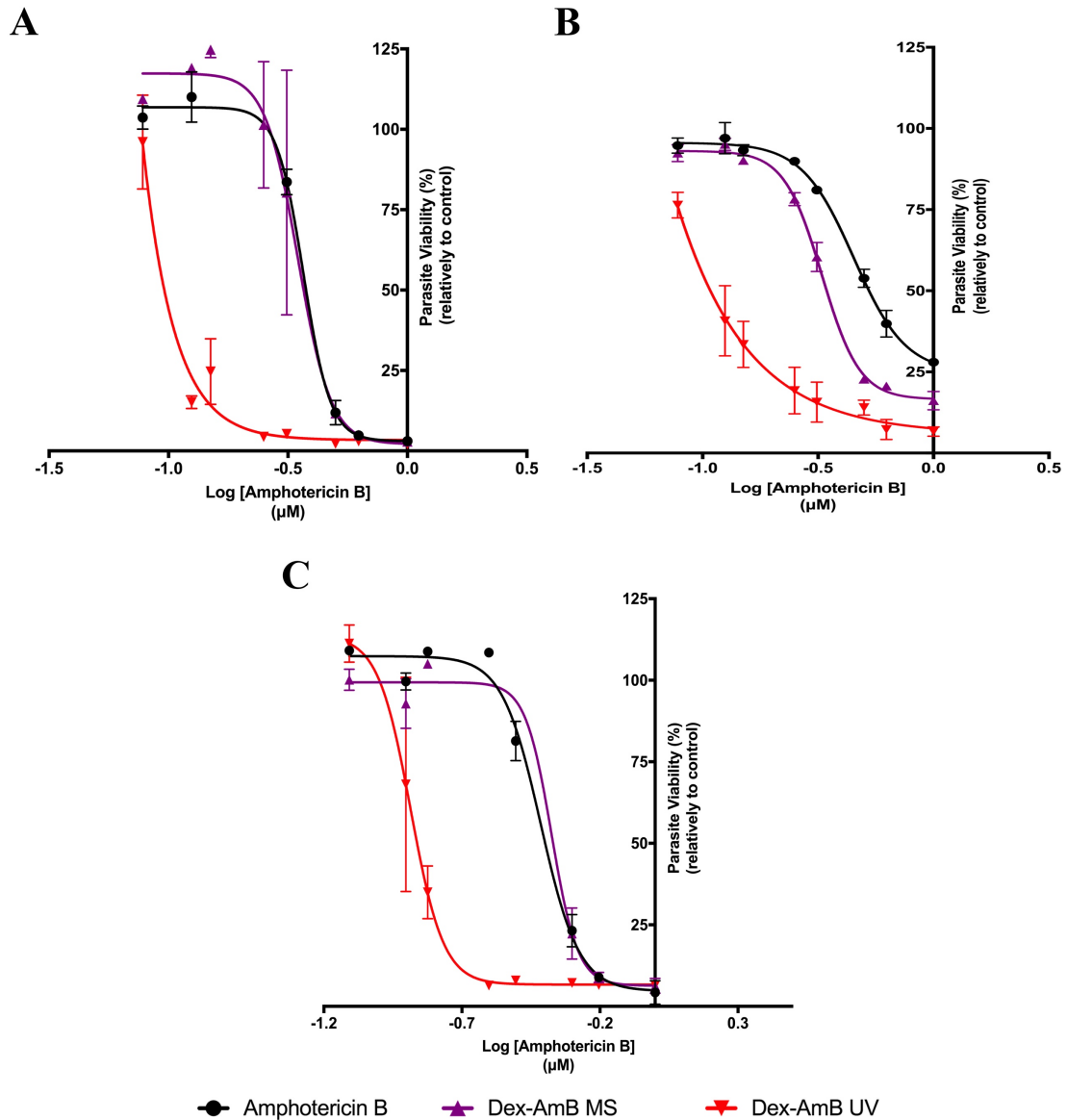
Figure 11- Evaluation of the anti-leishmanial effect of Dex-AmB formulation on the parasite viability of (A) *L. amazonensis* promastigotes, (B) *L. infantum* promastigotes, (C) *L. major* promastigotes and. Cells were incubated with the different concentrations of AmB and Dex-AmB for 24 h. After that period, parasite viability was evaluated by resazurin assay. Parasite viability is expressed in % relative to a control of parasites incubated only with culture media. Results are presented as mean ± SD (n=2).

Both the formulation and free-AmB promoted a decrease of around 50 % of the promastigote population when in concentrations between and 0.316 μM and 1 μM, presenting IC_{50} values of 0.3673 μM (AmB) and 0.3483 μM (Dex-AmB). In contrast, the IC_{50} value of the formulation based on the UV quantification was of 0.00869 μM (Figure 11A).

Alike what was seen for *L. amazonensis*, the dose-response curves of free-AmB and Dex-AmB formulation based on the MS quantification were the most similar for the two other *Leishmania* parasite strains. In the *L. major* promastigotes assay (Figure 11C), the IC_{50} values were of 0.3847 μM (AmB), 0.4212 μM (Dex-AmB MS) and 0.1302 μM (Dex-AmB UV). For *L. infantum* (Figure 11B), the IC_{50} values were of 0.4511 μM (AmB), 0.3286 μM (Dex-AmB MS) and 0.00087 μM (Dex-AmB UV).

It seems that the HPLC-UV method may somehow be underestimating the AmB content in the formulation, confirming the difficulties experimented while attempting to quantify AmB spectrophotometrically.

Overall, the results presented in this section appear to suggest that the quantification of AmB in the Dex-AmB formulation by HPLC-MS was more accurate than the one obtained using HPLC-UV. Therefore, we decided to use the developed HPLC-MS method to quantify the amount of AmB in the Dex-AmB formulation. The MS quantification results were further used throughout the biological assays in this work.

4.2.2   Hydrodynamic diameter and polydispersion index

When in aqueous solution, Dex-AmB formulation forms nanoparticles, owing to its amphiphilic character. Thus, in order to characterize our drug delivery system, hydrodynamic diameter and polydispersion index were analyzed using dynamic light scattering (DLS). These two parameters are of pivotal importance in the field of nanoparticles, since they will determine the *in vivo* distribution and drug release (R. Singh & Lillard, 2009). Furthermore, the hydrodynamic diameter is important to achieve a targeted delivery, where larger particle size will prompt an uptake by the MPS cells, allowing

the drug to reach the intracellular site where the parasite is confined (Akbari *et al.*, 2017; Gaumet *et al.*, 2008).

DLS, also known as photon correlation spectroscopy, is frequently used to measure nanoparticle properties. It is based on the particles' Brownian motion, which is directly influenced by the particle hydrodynamic diameter (Ramos, 2017; Stetefeld *et al.*, 2016).

Another relevant parameter to be assessed is the particle's homogeneity. DLS allows to obtain the Polydispersion index (PdI), a value of the particle hydrodynamic diameter distribution within the sample in analysis. PdI values range from 0 (perfectly homogeneous sample) to 1 (highly heterogeneous sample), with the first one being called monodisperse (narrow size distribution) and the latter being polydisperse (wider size distribution). Monomodal (one population) or plurimodal (numerous populations) particle size distribution can also be identified (Danaei *et al.*, 2018; Gaumet *et al.*, 2008; Masarudin *et al.*, 2015).

Table 7 comprises the Z-average (mean diameter) and the polydispersity index (PdI) of Dex-AmB formulation and dextrin, before and after filtration, in dH_2O. Dex-AmB formulation and dextrin presented a diameter of 460 nm and 137 nm, respectively, before filtration. These results highlight that the association of AmB to dextrin prompts a significant increase in particle size. The filtration (performed to sterilize the material) led to a decrease of Dex-AmB and dextrin diameter to 142 nm and 79.4 nm, respectively. No data regarding the hydrodynamic diameter of polysaccharide-based AmB formulations is available in literature, but both formulations (before and after filtration) are within the nano-size range (1 to 1000 nm) (R. Singh & Lillard, 2009).

As for the homogeneity, was seen that the PdI of the Dex-AmB formulation before filtration (0.34) was slightly above the recommended (<0.2) for polymer-based formulations (Danaei *et al.*, 2018), whereas after filtration, the PdI value (0.18) decreased to recommended values. Similarly, the PdI values of dextrin also decreased after filtration, from 0.28 to 0.26.

After filtration, AmB seemed to be retained in the filter.

44

Table 7- Average diameter and polydispersion index (PdI) of Dex-AmB and Dextrin nanoparticles in dH_2O, before and after filtration. Results are presented as mean ± SD (n=3)

Sample		Z-average (nm)	PdI
Dex-AmB	Before filtration	460.4 ± 46.3	0.34 ± 0.06
	After filtration	142.1 ± 3.1	0.18 ± 0.02
Dextrin	Before filtration	137.0 ± 8.3	0.28 ± 0.01
	After filtration	79.4 ± 3.2	0.26 ± 0.01

Using the zetasizer software, it is possible to plot size distribution by intensity or by volume, before and after filtration. These graphics allow to obtain further information on the formulation particles population and dispersity. Size distribution by intensity can be influenced by the presence of large particles, since it is based on the light scattering of each particle. Contrarily to this, size distribution by volume is based on the Mie theory, grouping the particles according to its volume or size, uncovering small populations of particles (Ramos, 2017; Stetefeld *et al.*, 2016). Figure 12 represents the size distribution by intensity and by volume of Dex-AmB formulation and dextrin, before and after filtration, in dH_2O.
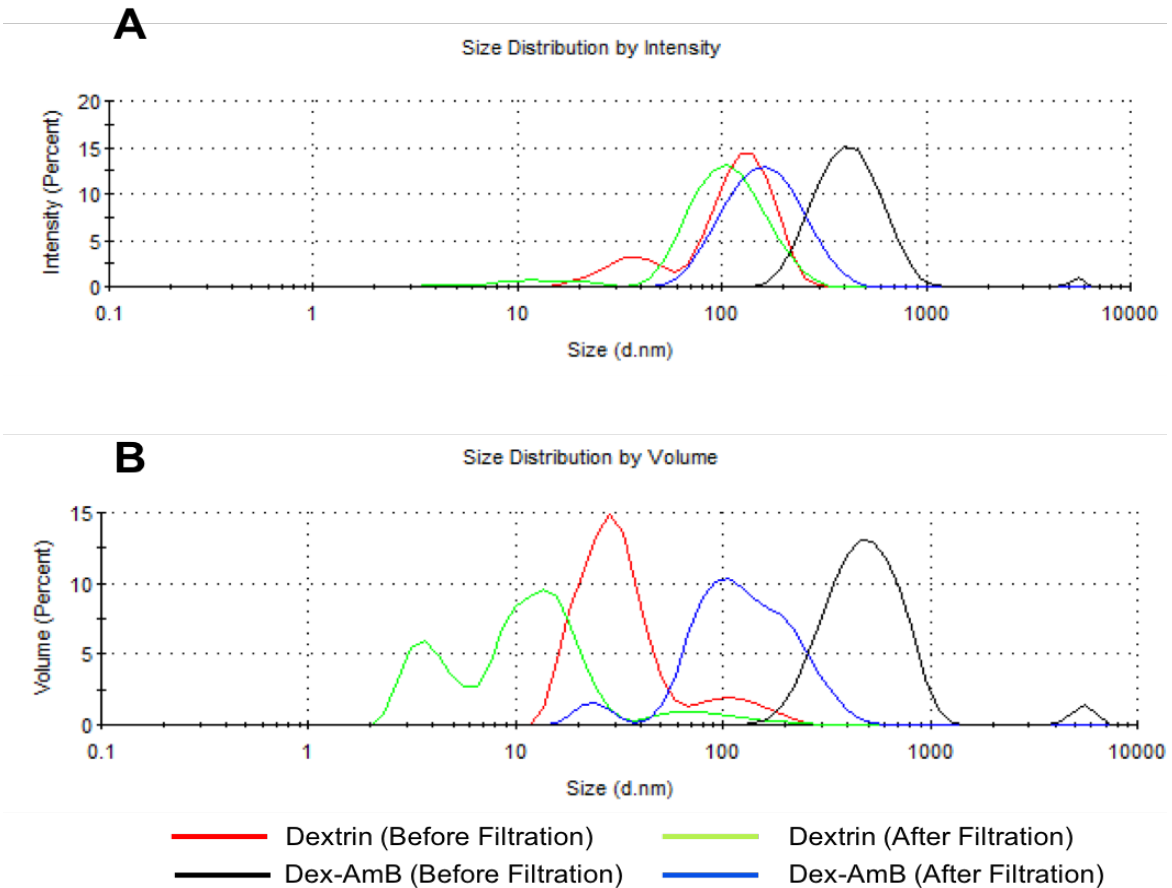
Figure 12- Size distribution by intensity (A) and volume (B) of the Dex-AmB formulation and dextrin in distilled water (dH$_2$O), before and after filtration. Results show the mean size of 3 repeated measurements of the same sample.

The graph of size distribution by intensity (Figure 12A) appears to indicate that, before filtration, Dex-AmB formulation (black curve) and dextrin (red curve) had a polydisperse distribution (two peaks). However, after filtration, Dex-AmB formulation (blue curve) and dextrin (green curve) appeared to present a monodisperse distribution (one peak), This is in accordance with the previously seen decrease in the PdI and appears to indicate that the filtration leads to a more homogeneous distribution of particles. Overall, when analysing the size distribution by intensity, Dex-AmB formulation and dextrin presented particle populations of above 400 nm and 100 nm (before filtration) and particle populations of above 200 nm and under 100 nm (after filtration), respectively. These results are in accordance with the Z-average and PdI values shown in Table 7, which are also intensity-based.

46

Using size distribution by volume (Figure 12B) the results appeared to be contradictory. Before filtration, the particle distribution appeared to be polydisperse for both samples, but unlike what was previously seen, after filtration, there were still different size populations, especially for dextrin. In this case, Dex-AmB formulation appeared to have large particle populations of above 400 nm before filtration. However, after filtration, a high volume of Dex-AmB particles appeared to have smaller size, slightly above 100 nm. As for dextrin, it presented major population of particles have a size under 100 nm before filtration and particles of less than 20 nm, divided in two populations, after filtration.

These results appear to support the theory that intensity-based distributions tend to give a greater relevance to large size particles, neglecting small size particle populations.

4.2.3   Particle size and particle concentration

Nanoparticle tracking analysis (NTA), is an alternative technique for size measurement that, similarly to DLS, is based on the Brownian motion of particles. However, this technique measures the particle-by-particle diffusion, instead of doing it from a bulk sample. With NTA is also possible to further observe and record the particles in solution and also overcome intensity-biased results seen with DLS. NTA measurements allowed to obtain the particle size and concentration in aqueous media, which were further compared with the previously described DLS results (Filipe *et al.*, 2010; Malloy, 2011).

Dex-AmB formulation displayed particle sizes of around 244 nm before filtration, with a particle concentration of 8.43×10^8 particles/mL in dH_2O (Table 8). When filtered, the size of Dex-AmB formulation decreased to 135 nm, with a particle concentration of 3.29×10^8 particles/mL (Table 8).

Table 8- Particle size and particle concentration of Dex-AmB formulation in distilled water (dH20), before and after filtration. Results are presented as mean ± SD (n=3)

Sample		Particle size (nm)	Particle concentration (particle/mL)
Dex-AmB	Before filtration	244 ± 122	8.43×10^8
	After filtration	135 ± 55	3.29×10^8

Figure 13 shows the plots obtained for Particle Size/Concentration of Dex-AmB formulation, before and after filtration, using the NanoSight software.
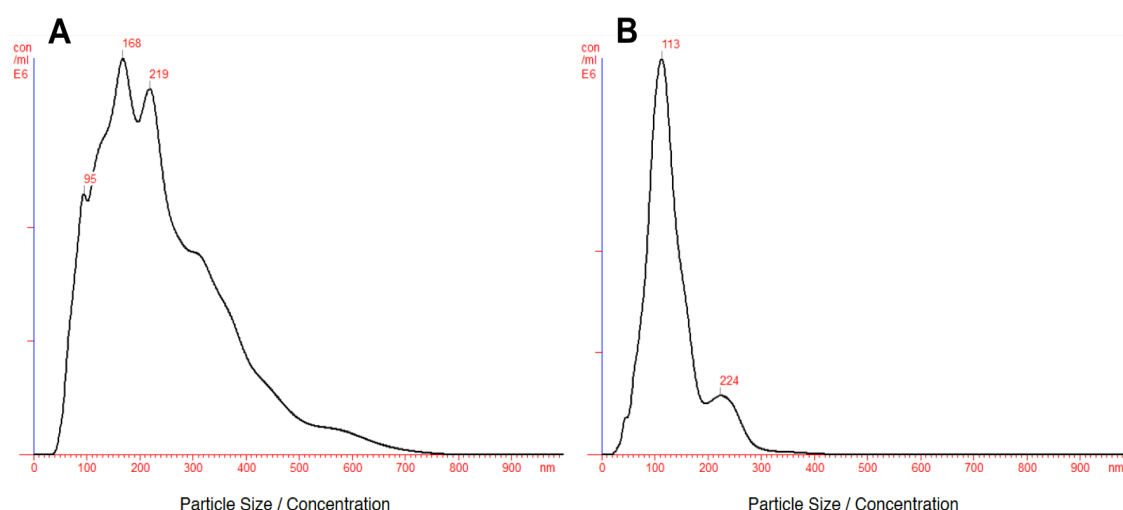
Figure 13- Dex-AmB formulation particle size and particle concentration (A) before filtration and (B) after filtration, in distilled water (dH$_2$O). Results show the mean size of 3 repeated measurements of the same sample.

Alike DLS intensity-based results, the formulation presented two main populations of particles, with two main peaks being observed at 168 nm and 219 nm. However, with NTA the mean particle size was considerably lower, and may better translate the real particle size value, since this technique is known for being more accurate when analysing polydisperse particle populations (Malloy, 2011). After filtration, the size and particle concentration decreased to around 113 nm and 3.29×10^8 particles/mL, respectively and the formulation appeared to be monodisperse. These results are in accordance with the ones obtained with DLS (intensity and volume-based size measurements) in the sense that both appear to indicate

that the filtration leads to a more homogeneous distribution of particles. However, we hypothesized that the decrease in particle concentration after filtration may be due to drug that is retained in the filter and is therefore, not available to form nanoparticles.

4.2.4 Cryo-Scanning Electron Microscopy

The results obtained in sections 4.2.2 and 4.2.3 were further confirmed using Cryo-Scanning Electron Microscopy (Cryo-SEM).
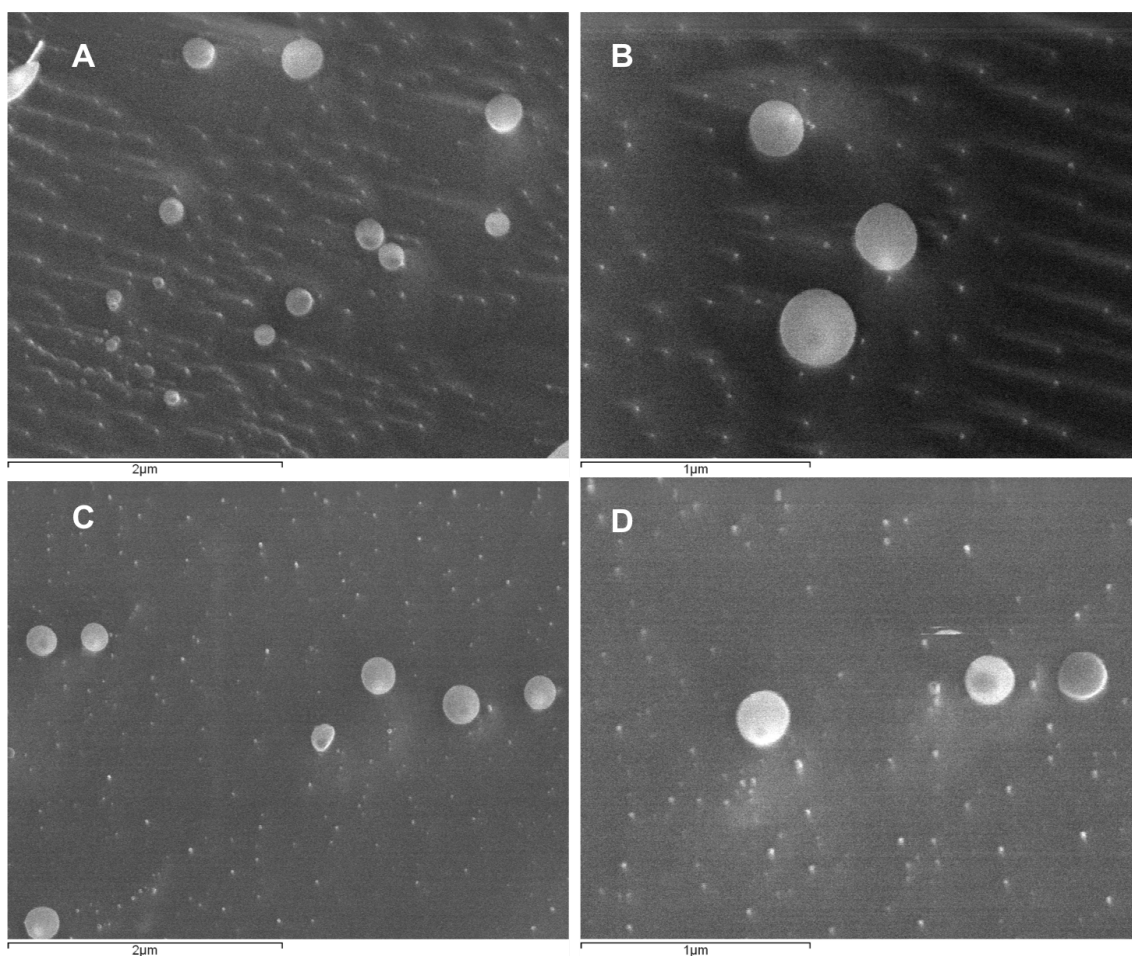
Figure 14- *Representative Cryo-scanning electron microscopy images at (A) 30000× (without filtration), (B) 500000× (without filtration), (C) 30000× (after filtration) and (D) 500000× (after filtration) magnification of Dex-AmB nanoparticles in distilled water (dH$_2$0) at a concentration of 2 mg/mL.*

When in aqueous solution (dH$_2$O), Dex-AmB formulation had a spherical morphology (Figure 12). These images (Figure 14C and 14D) appear to indicate that the filtration of the formulation does not result in a loss of shape, which remained spherical.

4.3 Cell and Parasite in vitro assays

4.3.1   Cytotoxicity to BMMφ

Considering that the nanoparticles are expected to be internalized by MPS cells, it is of major importance to ensure that the formulation does not present cytotoxic effects to these cells. Thus, the cytotoxic potential of the free-drug and Dex-AmB formulation was evaluated and the range of non-cytotoxic concentrations was determined. For this purpose, a primary culture of BMMφ was used. These cells are regarded as a suitable model to study resident macrophage's behaviour (Manzanero, 2012).

In order to assess the cell viability, a standard resazurin assay was performed. This method is based on the reduction of resazurin to resorufin by mitochondrial enzymes, which reflects the quantity of metabolically active cells (viable cells) (O'Brien *et al.*, 2000).

Firstly, the Dex-AmB formulation was tested, before and after filtration, with concentrations of AmB ranging from 1.56 to 50 μM. As seen in Figure 15C, the Dex-AmB formulation (before filtration) was cytotoxic only at the highest concentration tested (50 μM), causing the cell viability to decrease to under 70 %. Viability values under 70 % (red line) are usually regarded as denoting cytotoxicity potential ((ISO), 2009). Still, these data provides important information on the cytotoxic threshold of the formulation. The free-drug (Figure 15A) presented an identical cytotoxic profile, but the cell viability decreased to under 70 % when exposed to concentrations equal and higher than 25 μM. Dex-AmB formulation (after filtration) was safe at all tested concentrations, presenting a similar cytotoxic profile to dextrin (Figure 15B and 15D). More importantly, a visible difference in cell viability at 50 μM between non-filtered and filtered formulations was seen. The aforementioned reasons constitute a problem since, after filtering the Dex-AmB formulation, it will be impossible to know the concentration of the formulation due to a possible loss of material.
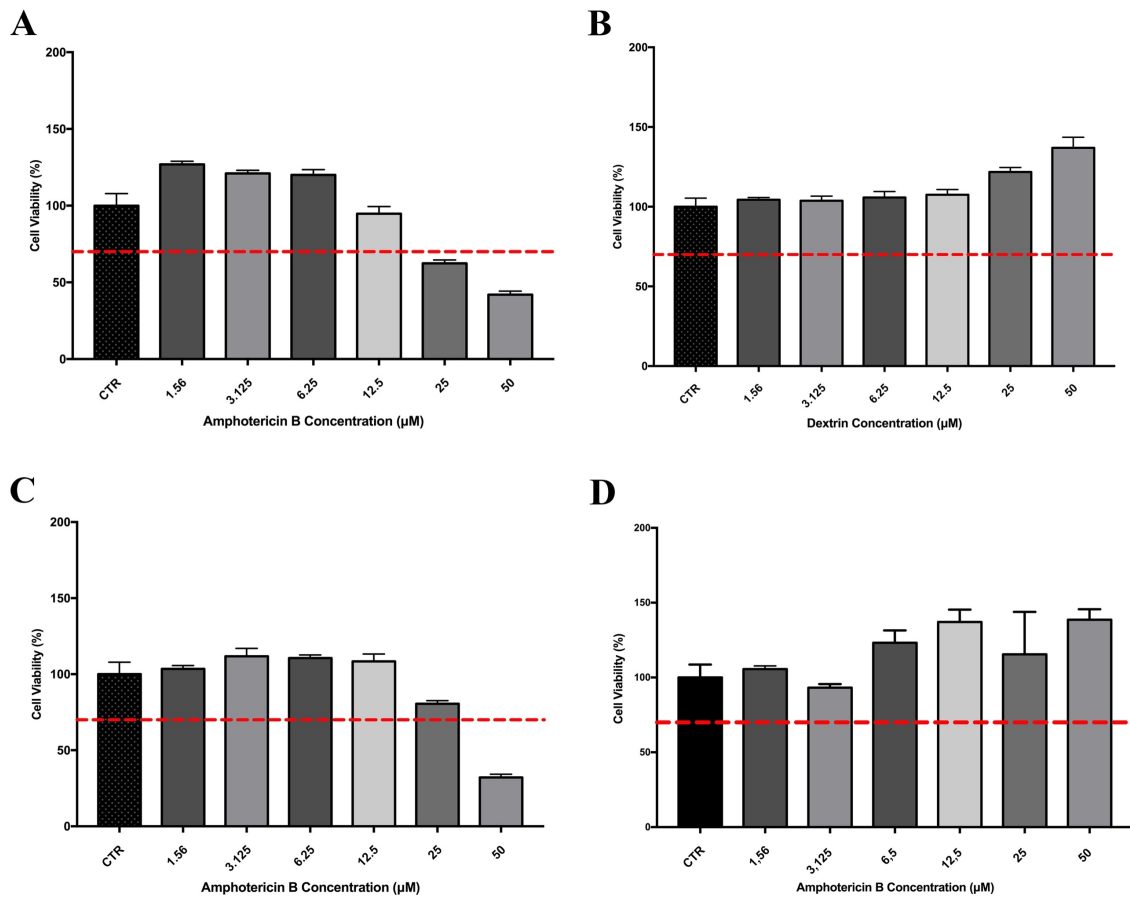
Figure 15- Viability of BMMϕ cells upon exposure, for 24h, to different concentrations of (A) Amphotericin B, (B) Dextrin, (C) Dex-AmB formulation (before filtration) and (D) Dex-AmB formulation (after filtration). Cell viability was evaluated by resazurin assay and is expressed in % relative to a control (CTR) of BMMϕ cells incubated only with culture media. The red line represents 70% viability. Results are presented as mean ± SD (n=2).

All the above led us into trying an alternative sterilization process to guarantee that our material was sterile when tested for its *in vitro* biocompatibility, while circumventing the likely loss of AmB seen when filtering the formulation. A sterilization process using ethylene oxide (EtO) was performed. This process is widely used to sterilize medical devices and polymers and is considered effective, since it does not promote physical changes of the material or an increase of its cytotoxicity (Franca *et al.*, 2013; Mendes *et al.*, 2007).

Afterwards, for free-AmB, dextrin and Dex-AmB formulation (sterile and non-sterile), concentrations ranging from 1.56 to 50 μM were assessed for their cytotoxic potential. Dextrin was apparently safe at all the tested concentrations (Figure 16B). These results are in accordance to what was

expected, since dextrin is generally recognized as safe (GRAS) by the FDA and previously developed dextrin-based formulations did not show cytotoxic potential against BMMϕ cells (Alvani *et al.*, 2011; Goncalves *et al.*, 2010). The viability values above 100 % seen for both formulations (non-sterile and sterile) and for dextrin may be explained by the cell growth stimulant character of dextrin (Asai *et al.*, 2011).
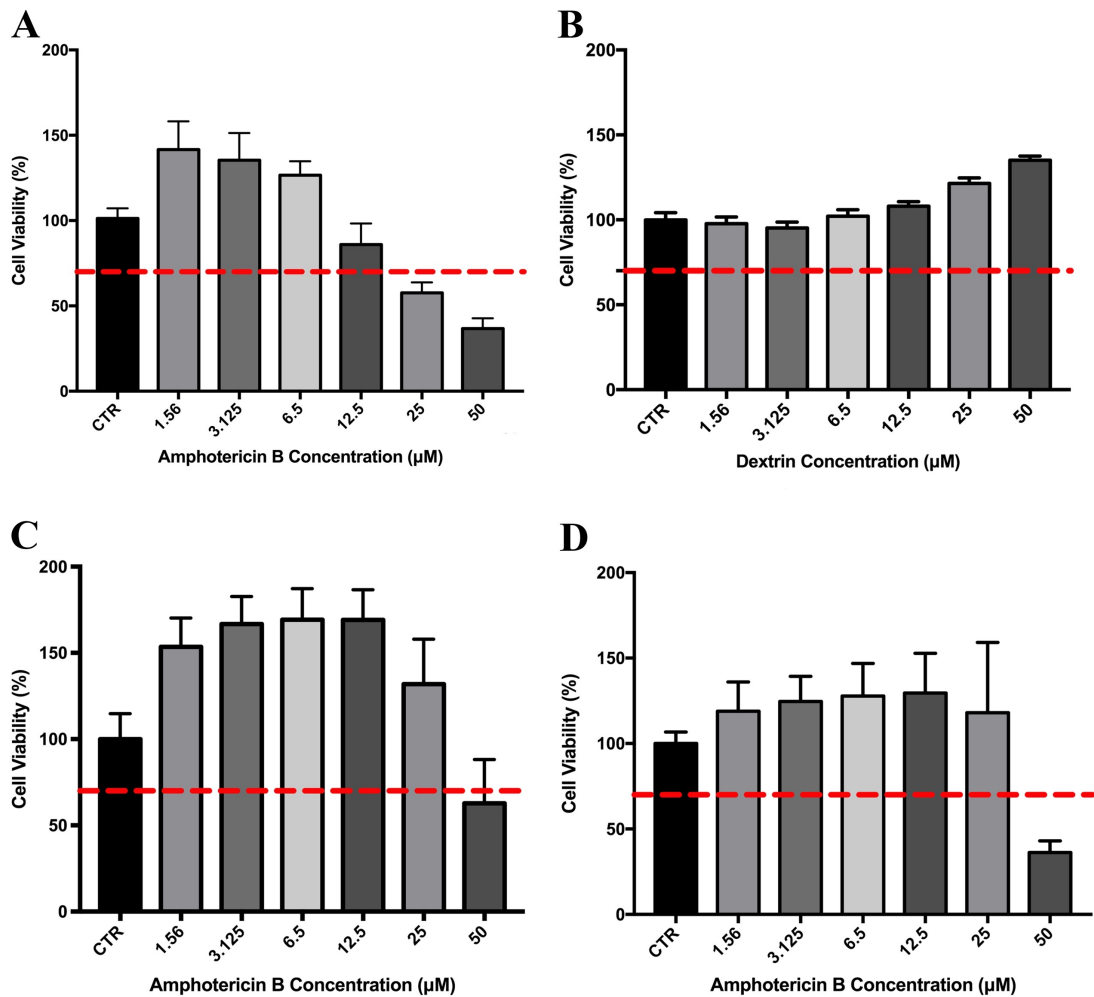
Figure 16- Viability of BMMϕ cells upon exposure, for 24h, to different concentrations of (A) Amphotericin B (AmB), (B) Dextrin, (C) Dex-AmB non-sterile and (D) Dex-AmB sterile. Cell viability was evaluated by resazurin assay and is expressed in % relative to a control (CTR) of BMMϕ cells incubated only with culture media. The red line represents 70% viability. Results are presented as mean ± SD (n=2).

Amphotericin B, in its free form, reduce the cell viability to levels under the 70 % threshold at concentrations between 12.5 and 25 μM (Figure 16A). The CC_{50} value was approximately 25 μM. These results are also in accordance with what is already reported in literature, since AmB was seen

to be toxic to mammalian cells (Kagan *et al.*, 2012) and to J774.2 murine macrophages at concentrations above 10 μM (Espuelas *et al.*, 2003) or 23.1 μM (Velasquez *et al.*, 2017). The sterilized formulation appears to be safe to macrophages in concentrations up to 25 μM of AmB, presenting mild toxicity at 50 μM, most likely due to the previously seen toxicity of AmB (Figure 16D). This appears to indicate that the association of AmB to dextrin is able to promote a reduction of the AmB cytotoxic effects towards BMMϕ when compared to the free-AmB. Thus, the CC_{50} value of our formulation is >25 μM. However, it must be remarked that under the conditions of the assay, AmB from the nanoformulation is likely to be released in the well, during the incubation time. On the other hand, if used *in vivo*, the nanoparticles are expected to reach their target before exerting systemic toxicity.

The EtO sterilization process did not markedly affect the cytotoxic profile of the formulation (as expected), but, similarly, to what was seen for the non-sterile formulation, the cell viability decreased when exposed to AmB concentrations of 50 μM (Figure 16C and 16D). Alike what was previously theorized, this toxicity was probably due to the cytotoxic character of AmB rather than the formulation.

Overall, the presented data appears to indicate that the Dex-AmB formulation is safe and may be used for macrophages targeting. More importantly, it seems that the conjugation of AmB to dextrin has a positive impact on the cytotoxic profile of AmB, reducing it.

4.3.2 Anti-leishmanial activity against axenic parasite cultures

The anti-leishmanial effect of the Dex-AmB formulation, AmB and dextrin was assessed using axenic cultures of *L. infantum* and *L. amazonensis* promastigotes. The parasites were exposed, during 24h, to concentrations ranging from 0.031 to 5 μM and, afterwards, the parasite viability was evaluated using a standard resazurin assay (Vale-Costa *et al.*, 2013).

Free-Amphotericin B reduces the *L. amazonensis* population by half when in concentrations between 0.1 and 0.316 μM. The 50% inhibitory concentration (IC_{50}) was of 0.2174 μM (Figure 17A). These results are in

accordance with values found in the literature (0.1 μM) (Chavez-Fumagalli *et al.*, 2015; Ribeiro *et al.*, 2014).
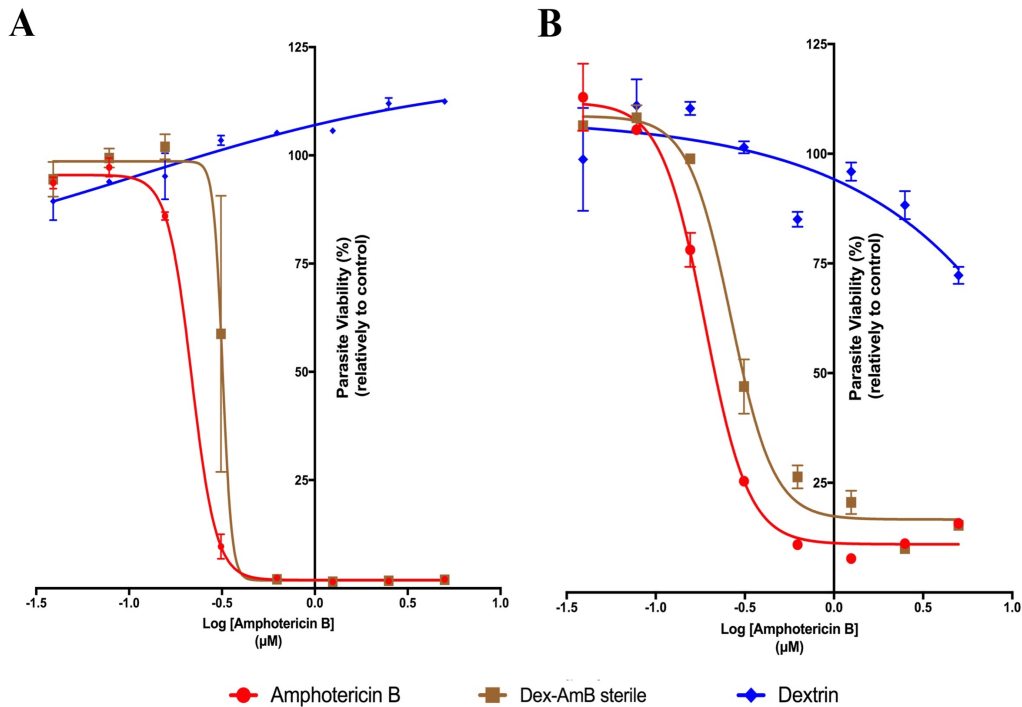
Figure 17 - Evaluation of the anti-leishmanial effect of Dex-AmB formulation sterile, AmB and Dextrin on the parasite viability of axenically grown (A) *L. amazonensis* promastigotes and (B) *L. infantum* promastigotes. Cells were exposed to the different concentrations of these compounds, for 24 h. After that period, parasite viability was evaluated by resazurin assay. Parasite viability is expressed in % relative to a control of parasites incubated only with culture media. Results are presented as mean ± SD (n=2).

Dextrin did not show any effect, as expected, for all the tested concentrations and strains. On the other hand, the Dex-AmB formulation (sterile form) also led to a decrease in the parasite viability, although slightly higher concentrations were required to do so, in comparison to the free-drug (Figure 17A), increasing the IC_{50} value to 0.3188 μM.

Similar results were obtained when the anti-leishmanial activity of the individual compounds was tested against axenic cultures of *L. infantum* promastigotes (Figure 17B). Free-AmB led to a 50 % reduction of the metabolically active parasites when in concentrations between 0.1 and 0.316 μM. For this *Leishmania* strain, the IC_{50} value of the free-drug was of 0.188 μM. This is close to the values described in the literature (0.22 μM) (Petri e Silva *et al.*, 2016).

The Dex-AmB formulation also displayed capacity to decrease parasite viability, as shown by its dose-response curve (Figure 17B). The IC_{50} obtained, 0.2645 µM, is slightly higher than the one of the free-drug.

Overall, these results show that the Dex-AmB formulation features anti-leishmanial activity against *L. amazonensis and L. infantum* promastigotes. However, these results were obtained using extracellular forms of the parasite and, thus, biological assays against intramacrophagic parasites are needed in order to draw more concise conclusions about the anti-leishmanial potential of the developed formulation.

4.3.3   Anti-leishmanial activity against intramacrophagic *L. infantum* and *L. amazonensis* amastigotes

The *in vitro* anti-leishmanial activity of free-AmB, Dex-AmB formulation (sterile form) and dextrin was evaluated on murine BMMϕ infected with *L. amazonensis* and *L. infantum* intracellular amastigotes. Concentrations ranging from 0.0313 µM to 1 µM were tested for all the compounds. A recently developed protocol (Gomes-Alves *et al.*, 2018) for InCell Analyzer was used and allowed to obtain the dose response curves for the tested compounds, as seen in Figure 18.
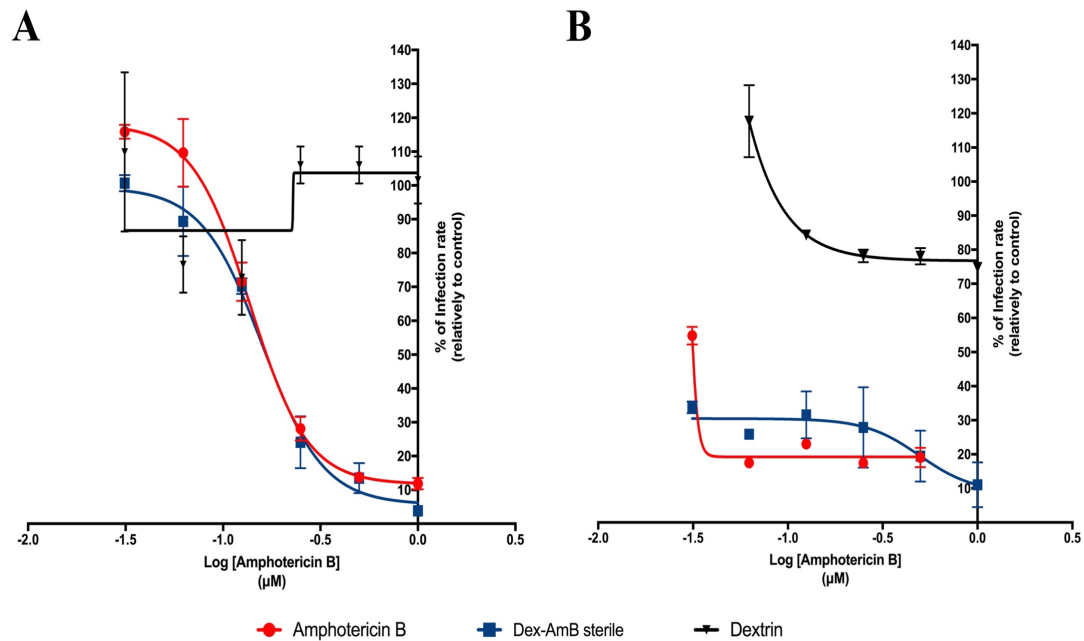
Figure 18- Evaluation of the anti-leishmanial effect of the Dex-AmB formulation (sterile form), AmB and Dextrin against (A) *L. amazonensis* intramacrophagic amastigotes and (B) *L. infantum* intramacrophagic amastigotes. Cells were exposed to the different concentrations of these compounds, for 24 h. Infection rate (%) (i.e., the quotient between the number of infected cells and the total number of cells, multiplied by 100) is expressed in relation to control intramacrophagic amastigotes incubated only with culture media. Results are presented as mean ± SD (n=2 for *L. amazonensis* and n=1 for *L. infantum*).

For the *L. amazonensis* intramacrophagic amastigotes, dextrin was not effective in reducing the infection rate because at all the tested concentrations the percentage of infection was always equal or above 90 % (Figure 18A). Free-AmB was able to eradicate half of the amastigote population when in concentrations between 0.1 μM and 0.316 μM. The 50% inhibitory concentration (IC_{50}) of free-AmB was of 0.1375 μM, but contradictory results on the IC_{50} may be found in literature, with some reporting IC_{50} of around 4.9 μM (Velasquez *et al.*, 2017) and others 0.06 μM (Ribeiro *et al.*, 2014).

The sterile Dex-Amb formulation had a similar anti-leishmanial activity to the free drug, promoting a decrease of around 50 % of the amastigote population when in concentrations between 0.1 μM and 0.316 μM. The IC_{50} of our formulation was of 0.1598 μM.

In parallel, the anti-leishmanial effect of the Dex-AmB, AmB and dextrin against *L. infantum* intramacrophagic amastigotes was assessed

(Figure 18B). However, these results were of only one independent experiment (n = 1), in which the percentage of infected BMMφ was extremely low ($\cong$ 30 %). Due to that, it was not possible to obtain dose-response curves or accurate IC_{50} values for AmB nor Dex-AmB. This assay should be repeated to assess the anti-leishmanial activity of our formulation against this specific parasite strain.

Nevertheless, we have previously shown that the Dex-AmB formulation was able to decrease the growth of *L. infantum* promastigotes to the same extent as the free-AmB. Although these results were for an extracellular form of the parasite, it was previously shown, in the literature, that free-AmB had a positive effect in reducing the burden of intramacrophagic *L. infantum* amastigotes (Gomes-Alves *et al.*, 2018; Petri e Silva *et al.*, 2016). Thus, and based on what was previously seen in the *L. amazonensis* intramacrophagic assay, it is expected that the formulation may be capable of promoting a release of AmB to *L. infantum*-infected macrophages.

Overall, the results presented in sections 4.3.1, 4.3.2 and 4.3.3, suggest that dextrin may be a suitable delivery system of AmB to *Leishmania*-infected macrophages, since the Dex-AmB formulation allows a decrease of drug toxicity to these mammalian cells while also displaying a similar *in vitro* anti-leishmanial potential to the free-drug.

4.4 Production of Dextrin-Amphotericin B Imine and Amine Conjugates

4.4.1   Degree of Oxidation (DO %) of oxidized dextrin

Oxidized dextrin was obtained by adapting a protocol of *Sokolsky-Papkov et al.* (2006). As seen in Table 9, this oxidation step had an overall yield of 78.8 %. Afterwards, the degree of oxidation (%) of OxDex was calculated using a modified protocol of Hydroxylamine hydrochloride titration described by Zhao & Heindel (1991). This colorimetric titration is based on the reaction between Hydroxylamine hydrochloride and the aldehydes in OxDex, which ends up forming a dextrin polyoxime and releasing a proton for each reacting aldehyde group. Afterwards, the solution is titrated with NaOH, in order to obtain the V_{NaOH} at the stoichiometric point

(Zhao & Heindel, 1991). Therefore, using the equations stated in the section 3.3.2, the OxDex had a degree of oxidation (%) of 16.1 % (Table 9).

Table 9- Overall yield (%) and degree of oxidation (%) of Oxidized dextrin

Sample	Overall yield (%)	Degree of Oxidation (%)
Oxidized Dextrin (OxDex)	78.8	16.1

This result is in accordance with what has been described by Sokolsky-Papkov *et al.* (2006), where they produced oxidized dextran with a degree of oxidation (%) of 15 %, by adding the same amount of potassium periodate to promote the oxidation of the polysaccharide.

4.4.2   Conjugation of Oxidized dextrin with AmB

Then, OxDex was conjugated with AmB, according to an adapted protocol of Sokolsky-Papkov *et al.* (2006), a method that has been reported to yield covalent conjugates of AmB in oxidized polysaccharides. The overall yield (%), AmB content (% w/w) and AmB Recovery Efficiency (%) were determined, using the HPLC-MS method as described above, scanning the range from 923 to 925 m/z (i.e., the free drug).

Table 10- Overall yield (%), AmB content (% w/w) and AmB recovery efficiency (%) of Imine Dex-AmB and Amine Dex-AmB formulations

Formulation	Overall yield (%)	AmB Content (% w/w)	AmB Recovery Efficiency (%)
ImDex-AmB conjugate	18.2	103.35 ± 2.23	94 ± 2.53
AmDex-AmB conjugate	20.5	100.13 ± 2.19	101 ± 2.76

Two conjugates were obtained using this protocol, which were supposedly formed through a Schiff base. The samples putatively corresponding to the imine Dex-AmB conjugate (ImDex-AmB) and the amine

Dex-AmB conjugate (AmDex-AmB), as described in the introduction section, presented an overall yield of 18.2 and 20.5 %, respectively (Table 10). These results were low when compared to the ones obtained by Ehrenfreund-Kleinman et al. (2002), who produced an arabinogalactan-AmB conjugate with an overall yield (%) of > 90% (for both amine and imine form), using the same protocol as the one apllied to produce the ImDex-AmB and AmDex-AmB conjugates. Moreover, the conjugates described in this section presented an overall yield that was almost four times lower than the one obtained for the Dex-AmB conjugate (71.1 %).

Regarding the AmB content (% w/w), the ImDex-AmB and AmDex-AmB conjugates presented 103.35 ± 2.23 % and 100.13 ± 2.19 % of AmB, respectively. However, these values correspond to free AmB. Since all of the AmB used in the preparation of the conjugates were detected in the free form (around 100% recovery), it may be concluded that the conjugation was merely through a self-assembling process, with no covalent conjugates being produced. The AmB content in the polysaccharide-AmB conjugates reported in the literature are much lower: 26 % and 23 % for the imine and amine form of Arabinogalactan-AmB conjugate, respectively (Ehrenfreund-Kleinman et al., 2002); 36.6 % and 34.4 % for the imine and amine form of Dextran-AmB conjugate, respectively (Sokolsky-Papkov et al., 2006). However, these figures were estimated using a HPLC-UV method which, as has been shown above, underestimates the AmB content quantification (Ehrenfreund-Kleinman et al., 2002; Sokolsky-Papkov et al., 2006).

These results appear to indicate that the oxidation of the polysaccharide prior to its synthesis with AmB, does not constitute an advantage to the final formulation. In fact, based on the overall yield (%) results, these oxidation steps lead to a lower yield of the formulation, likely due to the additional number of processing steps.

5. Conclusions and Future Perspectives

The main goal of this work was to develop a water-soluble Dextrin-Amphotericin B (Dex-AmB) formulation to treat Leishmaniasis. We expected the newly developed formulation to promote an improved solubilization and targeted delivery of AmB to *Leishmania* host cells, while reducing its toxic effects.

Initially, small batches of the Dex-AmB formulation were successfully produced. That motivated us to do a scale-up batch of the Dex-AmB formulation which was also efficiently achieved.

An HPLC-UV and HPLC-MS method were also developed to allow the quantification of the amount of AmB in the Dex-AmB formulation. The HPLC-MS quantification method proved to be more selective and accurate in quantifying the drug, thus being more suitable for our purposes. Because of that, the HPLC-MS method was used throughout the work.

The developed formulation was characterized by Dynamic light scattering, Nanoparticle Tracking Analysis and Cryo-Scanning Electron Microscopy. We demonstrated that the formulation was able to form spherical particles, when in aqueous solution. The nano-size of these particles was further confirmed, despite the discrepancies seen between the two size measurement techniques (e.g., DLS and NTA). Further investigation into this matter would be of interest. Nevertheless, the size of the formulation appears to be suitable for drug delivery, even though featuring some particle polydispersion.

The *in vitro* biocompatibility of the Dex-AmB formulation was assessed in macrophages, which are known to be one of the main host cells of *Leishmania*. The developed formulation seems to possess low cytotoxicity towards BMMΦ, when compared with free-AmB. This fact advocates the potential safety of the proposed drug delivery system. Moreover, the reduced cytotoxic potential of the formulation could enable the *in vivo* administration of higher doses of the drug, without the toxic side effects normally attached to it.

The anti-leishmanial potential of the Dex-AmB formulation was also assessed against *Leishmania* axenic promastigotes and intramacrophagic promastigotes. When tested against an extracellular form (promastigote) of the parasite, the formulation led to a reduction of the parasite viability, similarly to what was seen for the free-drug. Furthermore, the developed formulation also displayed anti-leishmanial activity against intracellular parasites, reducing the infection rate alike the free-AmB. These results were especially pronounced against one of the causative species of cutaneous leishmaniasis (CL), namely *L. amazonensis*.

Finally, we produced two supposedly covalent bond versions of the Dextrin-Amphotericin B formulation, through a conventional pre-oxidation of the polysaccharide, as it was done by other researchers using polysaccharides. These conjugates presented a substantially lower overall yield (%) when compared to the Dex-AmB formulation. Additionally, the oxidation steps in the production of these covalent conjugates, seemed to promote a loss of dextrin along the production process, as evidenced by the AmB content (% w/w) of over 100% of AmDex-AmB and ImDex-AmB conjugates.

To summarize, the results obtained in this work have demonstrated that a pre-oxidation of dextrin is not needed to render a Dex-AmB formulation. Furthermore, this newly developed system could have a promising role in the delivery of AmB and, consequently, in the treatment of leishmaniasis.

Although the main objectives of the project were achieved, additional efforts are still required in order to address some questions that still remain unanswered. For instance, it would be important to validate the developed HPLC-MS quantification method for its use in future works involving AmB. This validation and further assessment of the HPLC-MS method would also be relevant to clarify the values (>100 %) of AmB recovery efficiency in the formulation. Besides that, it would be relevant to assess the interactions between dextrin and AmB that led to the formulation here developed. In this sense, Fourier-transform infrared spectroscopy (FTIR) could be performed in

order to detect newly formed absorption bands after the conjugation of AmB to dextrin, since this technique is capable of identifying strong chemical bonds (*e.g.* covalent bond). Another potentially pertinent assay would be the evaluation of the *in vitro* drug release from the Dex-AmB conjugate. Additionally, it would be interesting to understand the extent of the interactions between the developed drug delivery formulation and the host immune system. One possibility would be to do *in vitro* uptake studies in BMMΦ cells using fluorescence microscopy and activation studies (cell surface markers or intracellular cytokines).

Notwithstanding the significant results regarding the anti-leishmanial activity and biocompatibility of our Dex-AmB formulation, these studies should be repeated to increase the statistical significance and possibly drawn some more conclusions.

Finally, and in a more advanced stages of the development, *in vivo* studies should be performed, in order to assess the formulation biodistribution and the selective targeting of macrophage-rich organs. The cytotoxic potential to healthy mice should also be assessed, and further on, anti-leishmanial activity assays in infected animals should be performed.

6. References

(ISO), I. O. f. S. (2009). ISO 10993-5:2009. Biological evaluation of medical devices -- Part 5: Tests for in vitro cytotoxicity. In.

Akbari, M., Oryan, A., & Hatam, G. (2017). Application of nanotechnology in treatment of leishmaniasis: A Review. *Acta Trop, 172*, 86-90. doi:10.1016/j.actatropica.2017.04.029

Al-Salem, W., Herricks, J. R., & Hotez, P. J. (2016). A review of visceral leishmaniasis during the conflict in South Sudan and the consequences for East African countries. *Parasit Vectors, 9*, 460. doi:10.1186/s13071-016-1743-7

Alvani, K., Qi, X., & Tester, R. F. (2011). Use of carbohydrates, including dextrins, for oral delivery. *Starch - Stärke, 63*(7), 424-431. doi:doi:10.1002/star.201000110

Alvar, J., Velez, I. D., Bern, C., et al. (2012). Leishmaniasis worldwide and global estimates of its incidence. *PLOS ONE, 7*(5), e35671. doi:10.1371/journal.pone.0035671

Alves, F., Bilbe, G., Blesson, S., et al. (2018). Recent Development of Visceral Leishmaniasis Treatments: Successes, Pitfalls, and Perspectives. *Clin Microbiol Rev, 31*(4). doi:10.1128/CMR.00048-18

Armijos, R. X., Weigel, M. M., Calvopina, M., et al. (2004). Comparison of the effectiveness of two topical paromomycin treatments versus meglumine antimoniate for New World cutaneous leishmaniasis. *Acta Trop, 91*(2), 153-160. doi:10.1016/j.actatropica.2004.03.009

Asai, T., Hayashi, T., Kuroki, K., et al. (2011). In vitro biocompatibility of dextrin: the addition of a low concentration of dextrin in the medium promotes the cell activity of L929 mouse fibroblasts. *Cell Biol Int, 35*(6), 645-648. doi:10.1042/CBI20100264

Ashford, R. W. (1996). Leishmaniasis reservoirs and their significance in control. *Clin Dermatol, 14*(5), 523-532.

Baginski, M., Czub, J., & Sternal, K. (2006). Interaction of amphotericin B and its selected derivatives with membranes: molecular modeling studies. *Chem Rec, 6*(6), 320-332. doi:10.1002/tcr.20096

Banuls, A. L., Hide, M., & Prugnolle, F. (2007). Leishmania and the leishmaniases: a parasite genetic update and advances in taxonomy, epidemiology and pathogenicity in humans. *Adv Parasitol, 64*, 1-109. doi:10.1016/S0065-308X(06)64001-3

Baran, M., Borowski, E., & Mazerski, J. (2009). Molecular modeling of amphotericin B-ergosterol primary complex in water II. *Biophys Chem, 141*(2-3), 162-168. doi:10.1016/j.bpc.2009.01.010

Bashaye, S., Nombela, N., Argaw, D., et al. (2009). Risk factors for visceral leishmaniasis in a new epidemic site in Amhara Region, Ethiopia. *Am J Trop Med Hyg, 81*(1), 34-39.

Bates, P. A. (2007). Transmission of Leishmania metacyclic promastigotes by phlebotomine sand flies. *Int J Parasitol, 37*(10), 1097-1106. doi:10.1016/j.ijpara.2007.04.003

Bates, P. A., & Rogers, M. E. (2004). New insights into the developmental biology and transmission mechanisms of Leishmania. *Curr Mol Med, 4*(6), 601-609.

Belen, A., & Alten, B. (2006). Variation in life table characteristics among populations of Phlebotomus papatasi at different altitudes. *J Vector Ecol, 31*(1), 35-44.

Bennis, I., Thys, S., Filali, H., et al. (2017). Psychosocial impact of scars due to cutaneous leishmaniasis on high school students in Errachidia province, Morocco. *Infect Dis Poverty, 6*(1), 46. doi:10.1186/s40249-017-0267-5

Boltz-Nitulescu, G., Wiltschke, C., Holzinger, C., et al. (1987). Differentiation of rat bone marrow cells into macrophages under the influence of mouse L929 cell supernatant. *J Leukoc Biol, 41*(1), 83-91.

Bruni, N., Stella, B., Giraudo, L., et al. (2017). Nanostructured delivery systems with improved leishmanicidal activity: a critical review. *Int J Nanomedicine, 12*, 5289-5311. doi:10.2147/IJN.S140363

Bulbake, U., Doppalapudi, S., Kommineni, N., & Khan, W. (2017). Liposomal Formulations in Clinical Use: An Updated Review. *Pharmaceutics, 9*(2). doi:10.3390/pharmaceutics9020012

Burza, S., Croft, S. L., & Boelaert, M. (2018). Leishmaniasis. *The Lancet*. doi:10.1016/S0140-6736(18)31204-2

Carvalho, J., Gonçalves, C., Gil, A. M., & Gama, F. M. (2007). Production and characterization of a new dextrin based hydrogel. *European Polymer Journal, 43*(7), 3050-3059. doi:https://doi.org/10.1016/j.eurpolymj.2007.02.046

Casaccia, P., Ladogana, A., Xi, Y. G., et al. (1991). Measurement of the concentration of amphotericin B in brain tissue of scrapie-infected hamsters with a simple and sensitive method. *Antimicrob Agents Chemother, 35*(7), 1486-1488.

Chang, Y., Wang, Y. H., & Hu, C. Q. (2011). Simultaneous determination of purity and potency of amphotericin B by HPLC. *J Antibiot (Tokyo), 64*(11), 735-739. doi:10.1038/ja.2011.83

Charvalos, E., Tzatzarakis, M. N., Van Bambeke, F., et al. (2006). Water-soluble amphotericin B-polyvinylpyrrolidone complexes with maintained antifungal activity against Candida spp. and Aspergillus spp. and reduced haemolytic and cytotoxic effects. *J Antimicrob Chemother, 57*(2), 236-244. doi:10.1093/jac/dki455

Chattopadhyay, A., & Jafurulla, M. (2011). A novel mechanism for an old drug: amphotericin B in the treatment of visceral leishmaniasis. *Biochem Biophys Res Commun, 416*(1-2), 7-12. doi:10.1016/j.bbrc.2011.11.023

Chavez-Fumagalli, M. A., Ribeiro, T. G., Castilho, R. O., et al. (2015). New delivery systems for amphotericin B applied to the improvement of leishmaniasis treatment. *Rev Soc Bras Med Trop, 48*(3), 235-242. doi:10.1590/0037-8682-0138-2015

Chawla, B., Jhingran, A., Panigrahi, A., et al. (2011). Paromomycin affects translation and vesicle-mediated trafficking as revealed by proteomics

of paromomycin -susceptible -resistant Leishmania donovani. *PLOS ONE, 6*(10), e26660. doi:10.1371/journal.pone.0026660

Colmenares, M., Kar, S., Goldsmith-Pestana, K., & McMahon-Pratt, D. (2002). Mechanisms of pathogenesis: differences amongst Leishmania species. *Trans R Soc Trop Med Hyg, 96 Suppl 1*, S3-7.

Danaei, M., Dehghankhold, M., Ataei, S., et al. (2018). Impact of Particle Size and Polydispersity Index on the Clinical Applications of Lipidic Nanocarrier Systems. *Pharmaceutics, 10*(2). doi:10.3390/pharmaceutics10020057

de Carvalho, R. F., Ribeiro, I. F., Miranda-Vilela, A. L., et al. (2013). Leishmanicidal activity of amphotericin B encapsulated in PLGA-DMSA nanoparticles to treat cutaneous leishmaniasis in C57BL/6 mice. *Exp Parasitol, 135*(2), 217-222. doi:10.1016/j.exppara.2013.07.008

de Menezes, J. P. B., Guedes, C. E. S., Petersen, A., et al. (2015). Advances in Development of New Treatment for Leishmaniasis. *BioMed Research International, 2015*, 11. doi:10.1155/2015/815023

de Souza, A., Marins, D. S. S., Mathias, S. L., et al. (2018). Promising nanotherapy in treating leishmaniasis. *Int J Pharm, 547*(1-2), 421-431. doi:10.1016/j.ijpharm.2018.06.018

de Vries, H. J., Reedijk, S. H., & Schallig, H. D. (2015). Cutaneous leishmaniasis: recent developments in diagnosis and management. *Am J Clin Dermatol, 16*(2), 99-109. doi:10.1007/s40257-015-0114-z

Debusk V, A. O. K., TN, US), Alleman, Tim (Knoxville, TN, US). (2006). United States Patent No.

Desbrieres, J., Peptu, C. A., Savin, C. L., & Popa, M. (2018). 10 - Chemically Modified Polysaccharides With Applications in Nanomedicine. In V. Popa & I. Volf (Eds.), *Biomass as Renewable Raw Material to Obtain Bioproducts of High-Tech Value* (pp. 351-399): Elsevier.

Dorlo, T. P., Balasegaram, M., Beijnen, J. H., & de Vries, P. J. (2012). Miltefosine: a review of its pharmacology and therapeutic efficacy in the treatment of leishmaniasis. *J Antimicrob Chemother, 67*(11), 2576-2597. doi:10.1093/jac/dks275

Dujardin, J. C., Campino, L., Canavate, C., et al. (2008). Spread of vector-borne diseases and neglect of Leishmaniasis, Europe. *Emerg Infect Dis, 14*(7), 1013-1018. doi:10.3201/eid1407.071589

Egger, P., Bellmann, R., & Wiedermann, C. J. (2001). Determination of amphotericin B, liposomal amphotericin B, and amphotericin B colloidal dispersion in plasma by high-performance liquid chromatography. *J Chromatogr B Biomed Sci Appl, 760*(2), 307-313.

Ehrenfreund-Kleinman, T., Azzam, T., Falk, R., et al. (2002). Synthesis and characterization of novel water soluble amphotericin B-arabinogalactan conjugates. *Biomaterials, 23*(5), 1327-1335.

Ehrenfreund-Kleinman, T., Golenser, J., & Domb, A. J. (2004). Conjugation of amino-containing drugs to polysaccharides by tosylation: amphotericin B-arabinogalactan conjugates. *Biomaterials, 25*(15), 3049-3057. doi:10.1016/j.biomaterials.2003.09.080

Eldem, T., & Arican-Cellat, N. (2000). High-performance liquid chromatographic determination of amphotericin B in a liposomal pharmaceutical product and validation of the assay. *J Chromatogr Sci, 38*(8), 338-344.

Ernst, C., Grange, J., Rinnert, H., et al. (1981). Structure of amphotericin B aggregates as revealed by UV and CD spectroscopies. *Biopolymers, 20*(8), 1575-1588. doi:doi:10.1002/bip.1981.360200802

Esch, K. J., & Petersen, C. A. (2013). Transmission and epidemiology of zoonotic protozoal diseases of companion animals. *Clin Microbiol Rev, 26*(1), 58-85. doi:10.1128/CMR.00067-12

Espada, R., Josa, J. M., Valdespina, S., et al. (2008). HPLC assay for determination of amphotericin B in biological samples. *Biomed Chromatogr, 22*(4), 402-407. doi:10.1002/bmc.947

Espuelas, M. S., Legrand, P., Campanero, M. A., et al. (2003). Polymeric carriers for amphotericin B: in vitro activity, toxicity and therapeutic efficacy against systemic candidiasis in neutropenic mice. *J Antimicrob Chemother, 52*(3), 419-427. doi:10.1093/jac/dkg351

Farber, S., Ickowicz, D., Sionov, E., et al. (2011). Galactomannan–amphotericin B conjugate: synthesis and biological activity. *Polymers for Advanced Technologies, 22*(1), 119-125. doi:doi:10.1002/pat.1874

Ferguson, E., Thomas, D., & Walsh, T. (2012). E. P. Office.

Filipe, V., Hawe, A., & Jiskoot, W. (2010). Critical evaluation of Nanoparticle Tracking Analysis (NTA) by NanoSight for the measurement of nanoparticles and protein aggregates. *Pharm Res, 27*(5), 796-810. doi:10.1007/s11095-010-0073-2

Franca, R., Mbeh, D. A., Samani, T. D., et al. (2013). The effect of ethylene oxide sterilization on the surface chemistry and in vitro cytotoxicity of several kinds of chitosan. *J Biomed Mater Res B Appl Biomater, 101*(8), 1444-1455. doi:10.1002/jbm.b.32964

Frézard, F., Demicheli, C., Da Silva, S. M., et al. (2017). Chapter 22 - Nanostructures for Improved Antimonial Therapy of Leishmaniasis. In A. M. Grumezescu (Ed.), *Nano- and Microscale Drug Delivery Systems* (pp. 419-437): Elsevier.

Gaumet, M., Vargas, A., Gurny, R., & Delie, F. (2008). Nanoparticles for drug delivery: the need for precision in reporting particle size parameters. *Eur J Pharm Biopharm, 69*(1), 1-9. doi:10.1016/j.ejpb.2007.08.001

Gershkovich, P., Wasan, E. K., Lin, M., et al. (2009). Pharmacokinetics and biodistribution of amphotericin B in rats following oral administration in a novel lipid-based formulation. *J Antimicrob Chemother, 64*(1), 101-108. doi:10.1093/jac/dkp140

Ghorbani, M., & Farhoudi, R. (2018). Leishmaniasis in humans: drug or vaccine therapy? *Drug Des Devel Ther, 12*, 25-40. doi:10.2147/DDDT.S146521

Gillespie, P. M., Beaumier, C. M., Strych, U., et al. (2016). Status of vaccine research and development of vaccines for leishmaniasis. *Vaccine, 34*(26), 2992-2995. doi:10.1016/j.vaccine.2015.12.071

Golenser, J., Frankenburg, S., Ehrenfreund, T., & Domb, A. J. (1999). Efficacious treatment of experimental leishmaniasis with amphotericin

B-arabinogalactan water-soluble derivatives. *Antimicrob Agents Chemother, 43*(9), 2209-2214.

Gomes, M. S., Sousa Fernandes, S., Cordeiro, J. V., et al. (2008). Engagement of Toll-like receptor 2 in mouse macrophages infected with Mycobacterium avium induces non-oxidative and TNF-independent anti-mycobacterial activity. *European Journal of Immunology, 38*(8), 2180-2189. doi:10.1002/eji.200737954

Gomes-Alves, A. G., Maia, A. F., Cruz, T., et al. (2018). Development of an automated image analysis protocol for quantification of intracellular forms of Leishmania spp. *PLOS ONE, 13*(8), e0201747. doi:10.1371/journal.pone.0201747

Goncalves, C., Torrado, E., Martins, T., et al. (2010). Dextrin nanoparticles: studies on the interaction with murine macrophages and blood clearance. *Colloids Surf B Biointerfaces, 75*(2), 483-489. doi:10.1016/j.colsurfb.2009.09.024

Gramiccia, M., & Gradoni, L. (2005). The current status of zoonotic leishmaniases and approaches to disease control. *Int J Parasitol, 35*(11-12), 1169-1180. doi:10.1016/j.ijpara.2005.07.001

Gupta, G., Oghumu, S., & Satoskar, A. R. (2013). Mechanisms of immune evasion in leishmaniasis. *Adv Appl Microbiol, 82*, 155-184. doi:10.1016/B978-0-12-407679-2.00005-3

Gupta, S., Pal, A., & Vyas, S. P. (2010). Drug delivery strategies for therapy of visceral leishmaniasis. *Expert Opin Drug Deliv, 7*(3), 371-402. doi:10.1517/17425240903548232

Gutierrez, V., Seabra, A. B., Reguera, R. M., et al. (2016). New approaches from nanomedicine for treating leishmaniasis. *Chem Soc Rev, 45*(1), 152-168. doi:10.1039/c5cs00674k

Handman, E., & Bullen, D. V. (2002). Interaction of Leishmania with the host macrophage. *Trends Parasitol, 18*(8), 332-334.

Herwaldt, B. L. (1999). Leishmaniasis. *Lancet, 354*(9185), 1191-1199. doi:10.1016/S0140-6736(98)10178-2

Hreczuk-Hirst, D., Chicco, D., German, L., & Duncan, R. (2001). Dextrins as potential carriers for drug targeting: tailored rates of dextrin degradation by introduction of pendant groups. *Int J Pharm, 230*(1-2), 57-66.

Iborra, S., Solana, J. C., Requena, J. M., & Soto, M. (2018). Vaccine candidates against leishmania under current research. *Expert Rev Vaccines, 17*(4), 323-334. doi:10.1080/14760584.2018.1459191

Ibrahim, F., Sivak, O., Wasan, E. K., et al. (2013). Efficacy of an oral and tropically stable lipid-based formulation of Amphotericin B (iCo-010) in an experimental mouse model of systemic candidiasis. *Lipids Health Dis, 12*, 158. doi:10.1186/1476-511X-12-158

Ickowicz, D. E., Farber, S., Sionov, E., et al. (2014). Activity, reduced toxicity, and scale-up synthesis of amphotericin B-conjugated polysaccharide. *Biomacromolecules, 15*(6), 2079-2089. doi:10.1021/bm5002125

Jain, J. P., & Kumar, N. (2010). Development of amphotericin B loaded polymersomes based on (PEG)(3)-PLA co-polymers: Factors affecting

size and in vitro evaluation. *Eur J Pharm Sci, 40*(5), 456-465. doi:10.1016/j.ejps.2010.05.005

Kagan, S., Ickowicz, D., Shmuel, M., et al. (2012). Toxicity mechanisms of amphotericin B and its neutralization by conjugation with arabinogalactan. *Antimicrob Agents Chemother, 56*(11), 5603-5611. doi:10.1128/AAC.00612-12

Kamhawi, S. (2006). Phlebotomine sand flies and Leishmania parasites: friends or foes? *Trends Parasitol, 22*(9), 439-445. doi:10.1016/j.pt.2006.06.012

Kaneo, Y., Taguchi, K., Tanaka, T., & Yamamoto, S. (2014). Nanoparticles of hydrophobized cluster dextrin as biodegradable drug carriers: solubilization and encapsulation of amphotericin B. *Journal of Drug Delivery Science and Technology, 24*(4), 344-351. doi:https://doi.org/10.1016/S1773-2247(14)50072-X

Kapil, S., Singh, P. K., & Silakari, O. (2018). An update on small molecule strategies targeting leishmaniasis. *Eur J Med Chem, 157*, 339-367. doi:10.1016/j.ejmech.2018.08.012

Karimi, A., Alborzi, A., & Amanati, A. (2016). Visceral Leishmaniasis: An Update and Literature Review. *Arch Pediatr Infect Dis, 4*(3), e31612. doi:10.5812/pedinfect.31612

Kaye, P., & Scott, P. (2011). Leishmaniasis: complexity at the host-pathogen interface. *Nat Rev Microbiol, 9*(8), 604-615. doi:10.1038/nrmicro2608

Kedzierski, L. (2010). Leishmaniasis Vaccine: Where are We Today? *J Glob Infect Dis, 2*(2), 177-185. doi:10.4103/0974-777X.62881

Kerr, D. J., Young, A. M., Neoptolemos, J. P., et al. (1996). Prolonged intraperitoneal infusion of 5-fluorouracil using a novel carrier solution. *Br J Cancer, 74*(12), 2032-2035.

Kothandaraman, G. P., Ravichandran, V., Bories, C., et al. (2017). Anti-fungal and anti-leishmanial activities of pectin-amphotericin B conjugates. *Journal of Drug Delivery Science and Technology, 39*, 1-7. doi:https://doi.org/10.1016/j.jddst.2017.02.010

Kreuter, J. (1991). Liposomes and nanoparticles as vehicles for antibiotics. *Infection, 19 Suppl 4*, S224-228.

Kumar, R., Sahoo, G. C., Pandey, K., et al. (2015). Study the effects of PLGA-PEG encapsulated amphotericin B nanoparticle drug delivery system against Leishmania donovani. *Drug Deliv, 22*(3), 383-388. doi:10.3109/10717544.2014.891271

Lakhal-Naouar, I., Slike, B. M., Aronson, N. E., & Marovich, M. A. (2015). The Immunology of a Healing Response in Cutaneous Leishmaniasis Treated with Localized Heat or Systemic Antimonial Therapy. *PLoS Negl Trop Dis, 9*(10), e0004178. doi:10.1371/journal.pntd.0004178

Laniado-Laborin, R., & Cabrales-Vargas, M. N. (2009). Amphotericin B: side effects and toxicity. *Rev Iberoam Micol, 26*(4), 223-227. doi:10.1016/j.riam.2009.06.003

Llanos-Cuentas, A., Echevarria, J., Cruz, M., et al. (1997). Efficacy of sodium stibogluconate alone and in combination with allopurinol for treatment of mucocutaneous leishmaniasis. *Clin Infect Dis, 25*(3), 677-684.

Lodge, R., & Descoteaux, A. (2008). Leishmania invasion and phagosome biogenesis. *Subcell Biochem, 47*, 174-181.

Lukes, J., Skalicky, T., Tyc, J., et al. (2014). Evolution of parasitism in kinetoplastid flagellates. *Mol Biochem Parasitol, 195*(2), 115-122. doi:10.1016/j.molbiopara.2014.05.007

Lux, H., Hart, D. T., Parker, P. J., & Klenner, T. (1996). Ether lipid metabolism, GPI anchor biosynthesis, and signal transduction are putative targets for anti-leishmanial alkyl phospholipid analogues. *Adv Exp Med Biol, 416*, 201-211.

Malloy, A. (2011). Count, size and visualize nanoparticles. *Materials Today, 14*(4), 170-173. doi:https://doi.org/10.1016/S1369-7021(11)70089-X

Manzanero, S. (2012). Generation of mouse bone marrow-derived macrophages. *Methods Mol Biol, 844*, 177-181. doi:10.1007/978-1-61779-527-5_12

Masarudin, M. J., Cutts, S. M., Evison, B. J., et al. (2015). Factors determining the stability, size distribution, and cellular accumulation of small, monodisperse chitosan nanoparticles as candidate vectors for anticancer drug delivery: application to the passive encapsulation of [(14)C]-doxorubicin. *Nanotechnol Sci Appl, 8*, 67-80. doi:10.2147/NSA.S91785

McConville, M. J., de Souza, D., Saunders, E., et al. (2007). Living in a phagolysosome; metabolism of Leishmania amastigotes. *Trends Parasitol, 23*(8), 368-375. doi:10.1016/j.pt.2007.06.009

Mendes, G. C., Brandao, T. R., & Silva, C. L. (2007). Ethylene oxide sterilization of medical devices: a review. *Am J Infect Control, 35*(9), 574-581. doi:10.1016/j.ajic.2006.10.014

Mendonca, D. V. C., Martins, V. T., Lage, D. P., et al. (2018). Comparing the therapeutic efficacy of different amphotericin B-carrying delivery systems against visceral leishmaniasis. *Exp Parasitol, 186*, 24-35. doi:10.1016/j.exppara.2018.02.003

Mesa-Arango, A. C., Scorzoni, L., & Zaragoza, O. (2012). It only takes one to do many jobs: Amphotericin B as antifungal and immunomodulatory drug. *Front Microbiol, 3*, 286. doi:10.3389/fmicb.2012.00286

Mohamed-Ahmed, A. H., Brocchini, S., & Croft, S. L. (2012). Recent advances in development of amphotericin B formulations for the treatment of visceral leishmaniasis. *Curr Opin Infect Dis, 25*(6), 695-702. doi:10.1097/QCO.0b013e328359eff2

Moradin, N., & Descoteaux, A. (2012). Leishmania promastigotes: building a safe niche within macrophages. *Front Cell Infect Microbiol, 2*, 121. doi:10.3389/fcimb.2012.00121

Moreira, S., Gil Da Costa, R. M., Guardão, L., et al. (2010). In Vivo Biocompatibility and Biodegradability of Dextrin-based Hydrogels. *Journal of Bioactive and Compatible Polymers, 25*(2), 141-153. doi:10.1177/0883911509357865

Mukhopadhyay, D., Dalton, J. E., Kaye, P. M., & Chatterjee, M. (2014). Post kala-azar dermal leishmaniasis: an unresolved mystery. *Trends Parasitol, 30*(2), 65-74. doi:10.1016/j.pt.2013.12.004

Murray, H. W., Berman, J. D., Davies, C. R., & Saravia, N. G. (2005). Advances in leishmaniasis. *Lancet, 366*(9496), 1561-1577. doi:10.1016/S0140-6736(05)67629-5

Naderer, T., & McConville, M. J. (2008). The Leishmania-macrophage interaction: a metabolic perspective. *Cell Microbiol, 10*(2), 301-308. doi:10.1111/j.1462-5822.2007.01096.x

Nagle, A. S., Khare, S., Kumar, A. B., et al. (2014). Recent developments in drug discovery for leishmaniasis and human African trypanosomiasis. *Chem Rev, 114*(22), 11305-11347. doi:10.1021/cr500365f

Nishi, K. K., Antony, M., Mohanan, P. V., et al. (2007). Amphotericin B-gum arabic conjugates: synthesis, toxicity, bioavailability, and activities against Leishmania and fungi. *Pharm Res, 24*(5), 971-980. doi:10.1007/s11095-006-9222-z

No, J. H. (2016). Visceral leishmaniasis: Revisiting current treatments and approaches for future discoveries. *Acta Trop, 155*, 113-123. doi:10.1016/j.actatropica.2015.12.016

Noronha, T. R. d., & Fock, R. A. (2018). Visceral leishmaniasis: amastigotes in the bone marrow. *Hematology, Transfusion and Cell Therapy*. doi:10.1016/j.htct.2018.06.003

O'Brien, J., Wilson, I., Orton, T., & Pognan, F. (2000). Investigation of the Alamar Blue (resazurin) fluorescent dye for the assessment of mammalian cell cytotoxicity. *European Journal of Biochemistry, 267*(17), 5421-5426. doi:doi:10.1046/j.1432-1327.2000.01606.x

Okwor, I., & Uzonna, J. (2016). Social and Economic Burden of Human Leishmaniasis. *Am J Trop Med Hyg, 94*(3), 489-493. doi:10.4269/ajtmh.15-0408

Olivier, M. (2011). Culprit within a culprit. *Nature, 471*, 173. doi:10.1038/471173a

Oryan, A., & Akbari, M. (2016). Worldwide risk factors in leishmaniasis. *Asian Pac J Trop Med, 9*(10), 925-932. doi:10.1016/j.apjtm.2016.06.021

Panaro, M. A., Panunzio, M., Jirillo, E., et al. (1995). Parasite escape mechanisms: the role of Leishmania lipophosphoglycan on the human phagocyte functions. A review. *Immunopharmacol Immunotoxicol, 17*(3), 595-605. doi:10.3109/08923979509016390

Pascual Martinez, F., Picado, A., Roddy, P., & Palma, P. (2012). Low castes have poor access to visceral leishmaniasis treatment in Bihar, India. *Trop Med Int Health, 17*(5), 666-673. doi:10.1111/j.1365-3156.2012.02960.x

Pavli, A., & Maltezou, H. C. (2010). Leishmaniasis, an emerging infection in travelers. *Int J Infect Dis, 14*(12), e1032-1039. doi:10.1016/j.ijid.2010.06.019

Peers, E., & Gokal, R. (1998). Icodextrin provides long dwell peritoneal dialysis and maintenance of intraperitoneal volume. *Artif Organs, 22*(1), 8-12.

Petri e Silva, S. C., Palace-Berl, F., Tavares, L. C., et al. (2016). Effects of nitro-heterocyclic derivatives against Leishmania (Leishmania) infantum promastigotes and intracellular amastigotes. *Exp Parasitol, 163*, 68-75. doi:10.1016/j.exppara.2016.01.007

Ponte-Sucre, A., Gamarro, F., Dujardin, J. C., et al. (2017). Drug resistance and treatment failure in leishmaniasis: A 21st century challenge. *PLoS Negl Trop Dis, 11*(12), e0006052. doi:10.1371/journal.pntd.0006052

Qin, W., Tao, H., Chen, Y., et al. (2012). Sensitive, accurate and simple liquid chromatography-tandem mass spectrometric method for the quantitation of amphotericin B in human or minipig plasma. *J Chromatogr Sci, 50*(7), 636-643. doi:10.1093/chromsci/bms049

Radwan, M. A., AlQuadeib, B. T., Siller, L., et al. (2017). Oral administration of amphotericin B nanoparticles: antifungal activity, bioavailability and toxicity in rats. *Drug Deliv, 24*(1), 40-50. doi:10.1080/10717544.2016.1228715

Ramos, A. P. (2017). 4 - Dynamic Light Scattering Applied to Nanoparticle Characterization. In A. L. Da Róz, M. Ferreira, F. de Lima Leite, & O. N. Oliveira (Eds.), *Nanocharacterization Techniques* (pp. 99-110): William Andrew Publishing.

Ravichandran, V., & Jayakrishnan, A. (2018). Synthesis and evaluation of anti-fungal activities of sodium alginate-amphotericin B conjugates. *Int J Biol Macromol, 108*, 1101-1109. doi:10.1016/j.ijbiomac.2017.11.030

Reithinger, R., Dujardin, J. C., Louzir, H., et al. (2007). Cutaneous leishmaniasis. *Lancet Infect Dis, 7*(9), 581-596. doi:10.1016/S1473-3099(07)70209-8

Ribeiro, T. G., Chavez-Fumagalli, M. A., Valadares, D. G., et al. (2014). Novel targeting using nanoparticles: an approach to the development of an effective anti-leishmanial drug-delivery system. *Int J Nanomedicine, 9*, 877-890. doi:10.2147/IJN.S55678

Rodrigues, C. D., Khalil, N. M., & Mainardes, R. M. (2014). Determination of amphotericin B in PLA-PEG blend nanoparticles by HPLC-PDA. *Brazilian Journal of Pharmaceutical Sciences, 50*, 859-868.

Rogers, M. E., Ilg, T., Nikolaev, A. V., et al. (2004). Transmission of cutaneous leishmaniasis by sand flies is enhanced by regurgitation of fPPG. *Nature, 430*(6998), 463-467. doi:10.1038/nature02675

Rosenthal, E., Delaunay, P., Jeandel, P. Y., et al. (2009). [Liposomal amphotericin B as treatment for visceral leishmaniasis in Europe, 2009]. *Med Mal Infect, 39*(10), 741-744. doi:10.1016/j.medmal.2009.05.001

Sadlova, J., Myskova, J., Lestinova, T., et al. (2017). Leishmania donovani development in Phlebotomus argentipes: comparison of promastigote- and amastigote-initiated infections. *Parasitology, 144*(4), 403-410. doi:10.1017/S0031182016002067

Saporito, L., Giammanco, G. M., De Grazia, S., & Colomba, C. (2013). Visceral leishmaniasis: host-parasite interactions and clinical presentation in the immunocompetent and in the immunocompromised host. *Int J Infect Dis, 17*(8), e572-576. doi:10.1016/j.ijid.2012.12.024

Seidi, F., Jenjob, R., Phakkeeree, T., & Crespy, D. (2018). Saccharides, oligosaccharides, and polysaccharides nanoparticles for biomedical applications. *J Control Release, 284*, 188-212. doi:10.1016/j.jconrel.2018.06.026

Serafim, C., Ferreira, I., Rijo, P., et al. (2016). Lipoamino acid-based micelles as promising delivery vehicles for monomeric amphotericin B. *Int J Pharm, 497*(1-2), 23-35. doi:10.1016/j.ijpharm.2015.11.034

Sereno, D., & Lemesre, J. L. (1997). Axenically cultured amastigote forms as an in vitro model for investigation of antileishmanial agents. *Antimicrobial Agents and Chemotherapy, 41*(5), 972-976.

Shabir, G. A. (2003). Validation of high-performance liquid chromatography methods for pharmaceutical analysis. Understanding the differences and similarities between validation requirements of the US Food and Drug Administration, the US Pharmacopeia and the International Conference on Harmonization. *J Chromatogr A, 987*(1-2), 57-66.

Silva, D. M., Nunes, C., Pereira, I., et al. (2014). Structural analysis of dextrins and characterization of dextrin-based biomedical hydrogels. *Carbohydr Polym, 114*, 458-466. doi:10.1016/j.carbpol.2014.08.009

Singh, O. P., Singh, B., Chakravarty, J., & Sundar, S. (2016). Current challenges in treatment options for visceral leishmaniasis in India: a public health perspective. *Infect Dis Poverty, 5*, 19. doi:10.1186/s40249-016-0112-2

Singh, O. P., & Sundar, S. (2014). Immunotherapy and targeted therapies in treatment of visceral leishmaniasis: current status and future prospects. *Front Immunol, 5*, 296. doi:10.3389/fimmu.2014.00296

Singh, R., & Lillard, J. W., Jr. (2009). Nanoparticle-based targeted drug delivery. *Exp Mol Pathol, 86*(3), 215-223. doi:10.1016/j.yexmp.2008.12.004

Sokolsky-Papkov, M., Domb, A. J., & Golenser, J. (2006). Impact of Aldehyde Content on Amphotericin B−Dextran Imine Conjugate Toxicity. *Biomacromolecules, 7*(5), 1529-1535. doi:10.1021/bm050747n

Souza, A. C., Nascimento, A. L., de Vasconcelos, N. M., et al. (2015). Activity and in vivo tracking of Amphotericin B loaded PLGA nanoparticles. *Eur J Med Chem, 95*, 267-276. doi:10.1016/j.ejmech.2015.03.022

Stanley, E. R., Chen, D. M., & Lin, H. S. (1978). Induction of macrophage production and proliferation by a purified colony stimulating factor. *Nature, 274*(5667), 168-170.

Stetefeld, J., McKenna, S. A., & Patel, T. R. (2016). Dynamic light scattering: a practical guide and applications in biomedical sciences. *Biophys Rev, 8*(4), 409-427. doi:10.1007/s12551-016-0218-6

Steverding, D. (2017). The history of leishmaniasis. *Parasit Vectors, 10*(1), 82. doi:10.1186/s13071-017-2028-5

Stockdale, L., & Newton, R. (2013). A review of preventative methods against human leishmaniasis infection. *PLoS Negl Trop Dis, 7*(6), e2278. doi:10.1371/journal.pntd.0002278

Stone, N. R., Bicanic, T., Salim, R., & Hope, W. (2016). Liposomal Amphotericin B (AmBisome((R))): A Review of the Pharmacokinetics, Pharmacodynamics, Clinical Experience and Future Directions. *Drugs, 76*(4), 485-500. doi:10.1007/s40265-016-0538-7

Strauss, G., & Kral, F. (1982). Borate complexes of amphotericin B: Polymeric species and aggregates in aqueous solutions. *Biopolymers, 21*(2), 459-470. doi:doi:10.1002/bip.360210216

Strazzulla, A., Cocuzza, S., Pinzone, M. R., et al. (2013). Mucosal Leishmaniasis: An Underestimated Presentation of a Neglected Disease. *BioMed Research International, 2013*, 7. doi:10.1155/2013/805108

Sundar, S., Jha, T. K., Thakur, C. P., et al. (2007). Injectable Paromomycin for Visceral Leishmaniasis in India. *New England Journal of Medicine, 356*(25), 2571-2581. doi:10.1056/NEJMoa066536

Tan, T. R., Hoi, K. M., Zhang, P., & Ng, S. K. (2016). Characterization of a Polyethylene Glycol-Amphotericin B Conjugate Loaded with Free AMB for Improved Antifungal Efficacy. *PLOS ONE, 11*(3), e0152112. doi:10.1371/journal.pone.0152112

Tiuman, T. S., Santos, A. O., Ueda-Nakamura, T., et al. (2011). Recent advances in leishmaniasis treatment. *Int J Infect Dis, 15*(8), e525-532. doi:10.1016/j.ijid.2011.03.021

Torres-Guerrero, E., Quintanilla-Cedillo, M. R., Ruiz-Esmenjaud, J., & Arenas, R. (2017). Leishmaniasis: a review. *F1000Res, 6*, 750. doi:10.12688/f1000research.11120.1

Vale-Costa, S., Gomes-Pereira, S., Teixeira, C. M., et al. (2013). Iron Overload Favors the Elimination of Leishmania infantum from Mouse Tissues through Interaction with Reactive Oxygen and Nitrogen Species. *PLOS Neglected Tropical Diseases, 7*(2), e2061. doi:10.1371/journal.pntd.0002061

van Griensven, J., Balasegaram, M., Meheus, F., et al. (2010). Combination therapy for visceral leishmaniasis. *Lancet Infect Dis, 10*(3), 184-194. doi:10.1016/S1473-3099(10)70011-6

Velasquez, A. M. A., Ribeiro, W. C., Venn, V., et al. (2017). Efficacy of a Binuclear Cyclopalladated Compound Therapy for Cutaneous Leishmaniasis in the Murine Model of Infection with Leishmania amazonensis and Its Inhibitory Effect on Topoisomerase 1B. *Antimicrob Agents Chemother, 61*(8). doi:10.1128/AAC.00688-17

Vijayakumar, S., & Das, P. (2018). Recent progress in drug targets and inhibitors towards combating leishmaniasis. *Acta Trop, 181*, 95-104. doi:10.1016/j.actatropica.2018.02.010

Walker, D. M., Oghumu, S., Gupta, G., et al. (2014). Mechanisms of cellular invasion by intracellular parasites. *Cell Mol Life Sci, 71*(7), 1245-1263. doi:10.1007/s00018-013-1491-1

Walker, K. Z., Gibson, J., Axiak, S. M., & Prentice, R. L. (1986). Potentiation of hybridoma production by the use of mouse fibroblast conditioned media. *J Immunol Methods, 88*(1), 75-81.

Wasan, E. K., Gershkovich, P., Zhao, J., et al. (2010). A novel tropically stable oral amphotericin B formulation (iCo-010) exhibits efficacy against visceral Leishmaniasis in a murine model. *PLoS Negl Trop Dis, 4*(12), e913. doi:10.1371/journal.pntd.0000913

Weigle, K., & Saravia, N. G. (1996). Natural history, clinical evolution, and the host-parasite interaction in New World cutaneous Leishmaniasis. *Clin Dermatol, 14*(5), 433-450.

WHO. (2007). *Report of a WHO informal consultation on liposomal amphotericin B*

in the treatment of visceral leishmaniasis. Retrieved from http://www.who.int/neglected_diseases/resources/AmBisomeReport.pdf.

WHO. (2010). *Control of the leishmaniases. World Health Organization technical report series.*

WHO. (2017a). *Global leishmaniasis update, 2006–2015: a turning point in leishmaniasis surveillance.* Retrieved from

WHO. (2017b). *Integrating neglected tropical diseases in global health and development.*

WHO. (2017c). UNVELING THE NEGLECT OF LEISHMANIASIS. Retrieved from http://www.who.int/leishmaniasis/Unveiling_the_neglect_of_leishmaniasis_infographic.pdf

WHO. (2018). Leishmaniasis and HIV coinfection. Retrieved from http://www.who.int/leishmaniasis/burden/hiv_coinfection/burden_hiv_coinfection/en/

Zhang, Y., Chan, J. W., Moretti, A., & Uhrich, K. E. (2015). Designing polymers with sugar-based advantages for bioactive delivery applications. *J Control Release, 219*, 355-368. doi:10.1016/j.jconrel.2015.09.053

Zhao, H., & Heindel, N. D. (1991). Determination of Degree of Substitution of Formyl Groups in Polyaldehyde Dextran by the Hydroxylamine Hydrochloride Method. *Pharmaceutical Research, 8*(3), 400-402. doi:10.1023/A:1015866104055

Zijlstra, E. E. (2016). The immunology of post-kala-azar dermal leishmaniasis (PKDL). *Parasites & Vectors, 9*(1), 464. doi:10.1186/s13071-016-1721-0